

Novel Scheme for Improving the Performance of a Wind Driven Doubly Fed Induction Generator During Grid Fault

Mahmoud A. Mossa and Yehia S. Mohamed

Electrical Engineering Department, Faculty of Engineering, El-Minia University, EL- Minia, Egypt
E-mail: eng_mahmoud2015@yahoo.com

Submitted August 13, 2011; Revised Nov 1, 2011, Accepted April 2, 2012.

ABSTRACT

Enhancement of fault ride-through (FRT) capability and subsequent improvement of rotor speed stability of wind farms equipped with doubly fed induction generator (DFIG) is the objective of this paper. The objective is achieved by employing a novel FRT scheme with suitable control strategy. The proposed FRT scheme, which is connected between the rotor circuit and dc link capacitor in parallel with Rotor Side Converter, consists of an uncontrolled rectifier, two sets of IGBT switches, a diode and an inductor. In this scheme, the input mechanical energy of the wind turbine during grid fault is stored and utilized at the moment of fault clearance, instead of being dissipated in the resistors of the crowbar circuit as in the existing FRT schemes. Consequently, torque balance between the electrical and mechanical quantities is achieved and hence the rotor speed deviation and electromagnetic torque fluctuations are reduced. This results in reduced reactive power requirement and rapid reestablishment of terminal voltage on fault clearance. Furthermore, the stored electromagnetic energy in the inductor is transferred into the dc link capacitor on fault clearance and hence the grid side converter is relieved from charging the dc link capacitor, which is very crucial at this moment, and this converter can be utilized to its full capacity for rapid restoration of terminal voltage and normal operation of DFIG. Extensive simulation study carried out employing MATLAB/SIMULINK software vividly demonstrates the potential capabilities of the proposed scheme in enhancing the performance of DFIG based wind farms to fault ride-through.

Keywords: DFIG, Fault ride-through (FRT), Low voltage ride-through (LVRT), Zero voltage ride-through (ZVRT), Rotor speed stability.

LIST OF SYMBOLS

V_{ds}^e, V_{qs}^e	d^e -axis and q^e -axis stator voltages.
i_{ds}^e, i_{qs}^e	d^e -axis and q^e -axis stator currents.
V_{dr}^e, V_{qr}^e	d^e -axis and q^e -axis rotor voltages.
i_{dr}^e, i_{qr}^e	d^e -axis and q^e -axis rotor currents.
i_{md}^e, i_{mq}^e	d^e -axis and q^e -axis magnetizing currents.
R_s	stator winding resistance, Ω .
R_r	rotor winding resistance, Ω .
L_m	magnetizing inductance, H .
L_s	stator self inductance, H .
L_r	rotor self inductance, H .

w_r	electrical rotor angular speed in rad./sec.
θ_e	electrical stator flux angle.
θ_r	electrical rotor angular position.
θ_{slip}	electrical slip flux angle.
T_e	electromagnetic torque, N.m.
I_{rdc}	rectified Rotor current, A.
R_{cw}	crowbar resistance, Ω .
t_f	fault duration, sec.
L	storage inductance, H.

I. INTRODUCTION

The use of renewable energy sources for electric power generation is gaining importance in order to reduce global warming and environmental pollution, in addition to meeting the escalating power demand of the consumers. Among various renewable energy technologies, grid integration of wind energy electric conversion system is being installed in huge numbers due to their clean and economical energy conversion [1]. Recent advancements in wind turbine technology and power electronic systems are also more instrumental for the brisk option of grid integration of wind energy conversion system [2]. Doubly fed induction generator (DFIG) based wind turbines offer more advantages such as operation over wide range of rotor speeds, four-quadrant active and reactive power control capabilities with improved efficiency compared to other wind turbine technologies [3]. With back to back pulse width modulated (PWM) converters connected in the rotor circuit of induction machine known as rotor side converter (RSC) and grid side converter (GSC), independent control of real power/speed and reactive power can be achieved by employing vector control method [4]. The main advantage of DFIG is that the converters carry only a fraction (25-30%) of the total power; hence the losses in the power electronic converters and their cost are considerably less.

In the past, the protection requirements of wind turbines were focused on safeguarding the turbines themselves. When the network suffers any transient disturbance such as voltage sag or short circuit fault, the wind turbine generators are usually disconnected from the grid as soon as the occurrence of voltage dip in the range of 70-80%. However, with large integration of wind generators in the power system network, loss of considerable part of wind generators following a transient disturbance is not preferable. Tripping of numerous wind generators during transient disturbance can further risk the stability of power system thereby contributing to amplification of the effect of the disturbance that has originated. According to recent grid code requirement [5, 6], wind generators should remain connected and actively support the grid during network fault or any other transient disturbance. Therefore, it has become inevitable for existing and new upcoming wind generators to be equipped with "fault ride-through (FRT) or low voltage ride-through (LVRT) or zero voltage ride through (ZVRT) schemes" to avoid their disconnection from the power system network during grid faults. Moreover, FRT is extremely important for maintaining system reliability and voltage stability, especially in areas where concentration of wind power generation facilities are high.

As a result of grid fault, the DFIG terminal voltage drops to a very low value, which is accompanied with increased stator current. The stator disturbance is further transmitted to the rotor because of magnetic coupling between the stator and rotor, thereby resulting in high transient rotor current. As the stator-rotor turns ratio of DFIG is chosen according to the

desired variable speed range, it may not be possible to obtain the required rotor voltage from RSC to control high rotor current during grid faults. Current control techniques are usually adopted to limit the rotor current, which however leads to high voltage at the converter terminals that may harm the RSC.

The traditional method to protect the RSC of DFIG is to short circuit the rotor windings using a "thyristor crowbar" circuit [7, 8]. Thyristor crowbar is usually made of anti-parallel thyristors or a diode bridge with anti-parallel thyristors and additional resistors if any needed. The external resistors are deployed to reduce the rotor current on fault occurrence and the reactive power requirement of the induction machine on fault clearance [9]. The thyristor crowbar is enabled and signals to RSC are blocked whenever the rotor current exceeds its limit. The crowbar and RSC recover to the pre-fault condition after the terminal voltage is restored above certain value following fault clearance. Hansen and Michalke have utilized power factory DIgSILENT, a power system simulation toolbox, to study the FRT capability of wind turbines [10]. A supplementary damping controller to damp the torsional oscillations in the wind turbine shaft that may affect the converter operation during grid faults was investigated. In addition, criteria for selection of size of crowbar resistance based on the parameters namely rotor current, electromagnetic torque and reactive power were demonstrated. The results of the analysis show that a small value of crow bar resistance causes high rotor current and torque transient peaks at the fault moment. A high value of crow bar resistance can however imply a risk of excessive transients in rotor current, electromagnetic torque and reactive power at the instant of removal of crowbar circuit. In [11], a soft transition from transient condition to normal operation with thyristor crowbar circuit is attempted by setting the reference values for the controllers equal to the values of currents at the moment of fault clearance. These values are then slowly ramped up to the required reference values. In spite of the above, with thyristor crowbar scheme, transients could not be avoided at the resumption of normal operation.

Seman et al. have proposed an active crowbar circuit employing fully controllable bidirectional switches to protect the converters of DFIG [12]. The operation of active crow bar is controlled by dc link voltage. However, the dc link voltage alone is not a suitable candidate for the control of active crow bar circuit as it does not reflect the increase in rotor current under all situations. An additional anti-parallel thyristor switch in the stator circuit to limit the stator current subsequent to the instant of fault clearing was proposed in [13]. This method requires an additional switch with the rating of stator circuit and also it disconnects the stator winding during fault and completely interrupts stator active power generation. The impediment situation in all the above solution methods is troublesome evacuation of heat generated in the resistors of the crowbar circuit for a long-duration voltage sag or interruption. Moreover, the speed deviation that is resulted by a grid disturbance could not be averted in both thyristor and active crowbar FRT schemes. Hence with the above schemes, the reactive power requirement of DFIG at the instant of fault clearance is higher than the pre-fault value.

In this paper, a novel FRT scheme is proposed. In this scheme, the input mechanical energy of the wind turbine during grid fault is stored and utilized at the moment of fault clearance, instead of being dissipated in the resistors of the crowbar circuit as in the existing FRT schemes. The proposed FRT scheme, which is connected between the rotor circuit and dc link capacitor in parallel with RSC, consists of an uncontrolled rectifier, two sets of IGBT switches, a diode and an inductor. As these components are rated for rotor circuit power ratings, the proposed scheme is cost effective.

The objective of the proposed scheme which employs minimal additional hardware components and simple control technique for successful fault ride-through of DFIG are:

- Satisfactory performance and compliance with grid code requirements.
- Protection of generator converters against over-current and dc link capacitor against excessive over-voltage.
- Enhancing the stability of DFIG by damping speed deviations and electromagnetic torque fluctuations.
- Reduction of reactive power requirement of DFIG with rapid reestablishment of terminal voltage at fault clearance.

The rest of the paper is organized into following sections. Basic control structure and operation of DFIG is briefly presented in the next section. In Section 3, the proposed FRT scheme with a suitable control technique for performance enhancement of DFIG is presented. An extensive analysis and performance evaluation of proposed FRT scheme under single line to ground fault condition at the generator terminals is carried out by simulation using MATLAB/SIMULINK software, which is presented in Section 4. The imperative results obtained with the proposed FRT scheme are included in the concluding remark.

2. BASIC CONTROL STRUCTURE AND OPERATION OF DFIG

The basic control structure of DFIG is shown in Fig. 1. The wind turbine drives the rotor of DFIG through a set of low/high speed gear box mechanical system. The stator of the DFIG is directly connected to the grid through a step up transformer, while the rotor is connected to the grid through back to back insulated gate bipolar junction transistor (IGBT) pulse width modulated (PWM) converters with a common dc link capacitor. In the present analysis, the entire system is modeled in a synchronously rotating d-q reference frame for achieving decoupled control of real and reactive powers of DFIG. Since the objective of this paper is primarily to enhance the FRT capabilities of DFIG, the authors suggest the readers to refer to the past literatures [6, 15-18], for computer modeling of DFIG.

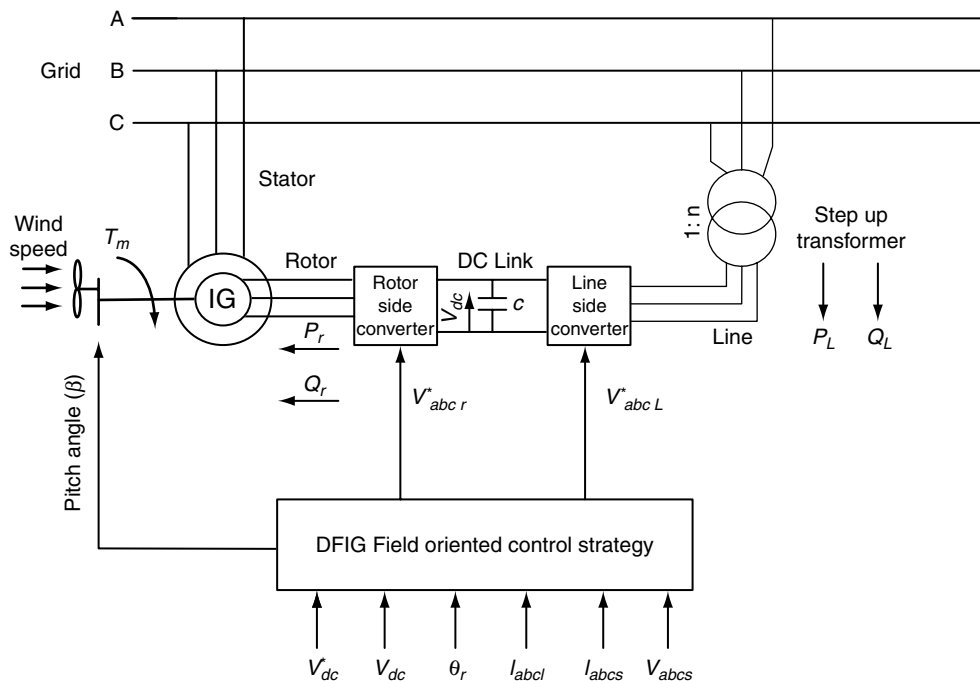


Figure 1: Basic control structure of grid connected DFIG.

The field orientation techniques allow decoupled or independent control of both active and reactive power. These techniques are based on the concept of d^e-q^e controlling in different reference frames [14], where the current and the voltage are decomposed into distinct components related to the active and reactive power. In this work, the stator flux oriented rotor current control, with decoupled control of active and reactive power is adopted.

The control schemes for the doubly-fed induction machine are expected to track a prescribed maximum power curve, for maximum power capturing and to be able to control the reactive power generation. These control objectives must be achieved with adequate stability of the system which also includes the power converter and the dc link. The total active and reactive power generated can be calculated in terms of d^e-q^e stator voltage and current components as [15]

$$P_s = \frac{3}{2} |V_s| i_{qs}^e \quad (1)$$

$$Q_s = \frac{3}{2} |V_s| i_{ds}^e \quad (2)$$

Where

$$|V_s| = \sqrt{\left((V_{ds}^e)^2 + (V_{qs}^e)^2\right)}$$

The field orientation control is based on the field d^e-q^e model, where the reference frame rotates synchronously with respect to the stator flux linkage, with the d-axis of the reference frame instantaneously overlaps the axis of the stator flux. By aligning the stator flux phasor λ_s on the d^e - axis, so ($\omega = \omega_e$ and $\lambda_{qs}^e = 0$, $\lambda_{ds}^e = \lambda_s$). In such case the following expressions are obtained

$$\begin{aligned} \lambda_{qs}^e &= L_s i_{qs}^e + L_m i_{qr}^e = 0 \\ \therefore i_{qs}^e &= -\frac{L_m}{L_s} i_{qr}^e \end{aligned} \quad (3)$$

The developed electromagnetic torque can be expressed in terms of $d^e - q^e$ stator current and flux components as:

$$T_e = \frac{3}{2} \frac{P}{i_{qs}^e \lambda_{ds}^e - i_{ds}^e \lambda_{qs}^e} \quad (4)$$

By putting $\lambda_{qs}^e = 0$, in the torque equation, this yields:

$$\therefore T_e = \frac{3}{2} \frac{P}{i_{qs}^e \lambda_{ds}^e} \quad (5)$$

Using (3) and the active power equation (1), the equation of the active power becomes:

$$P_s = -\frac{3}{2} |V_s| \frac{L_m}{L_s} i_{qr}^e \quad (6)$$

The d^e -axis stator current component can be written as

$$\begin{aligned} i_{ds}^e &= i_{md}^e - i_{dr}^e \\ &= \frac{|V_s|}{2\pi f_s L_m} - i_{dr}^e \end{aligned} \quad (7)$$

Using (7) and the reactive power equation (2), the equation of the reactive power can be expressed as follows:

$$Q_s = \frac{3}{2}|V_s| \left(\frac{|V_s|}{2\pi f_s L_m} - i_{dr}^e \right) \quad (8)$$

Therefore, the d^e -axis rotor current component, (i_{dr}^e) can be obtained by regulating the stator reactive power. On the other hand, the q^e -axis rotor current component, (i_{qr}^e) can be obtained to regulate the stator active power and the generator speed [15, 16]. As a result, the control of the stator active power (P_s) via (i_{qr}^e) as shown in Fig. 2 and the control of the stator reactive power (Q_s) via (i_{dr}^e) as shown in Fig. 3 are essentially decoupled, and so a separate decoupler is not necessary to implement field orientation control for the slip power recovery. Flux control is generally unnecessary, (since it would maintain a constant level, restricted by the constant magnitude and frequency of the line voltage), while the control of reactive power becomes possible.

The stator flux linkage components in the stationary stator reference frame can be calculated through the integration of the difference between the phase voltage and the voltage drop in the stator resistance as;

$$\begin{aligned} \lambda_{ds}^s &= \int [(V_{ds}^s - i_{ds}^s R_s) dt \\ \lambda_{qs}^s &= \int [(V_{qs}^s - i_{qs}^s R_s) dt \end{aligned} \quad (9)$$

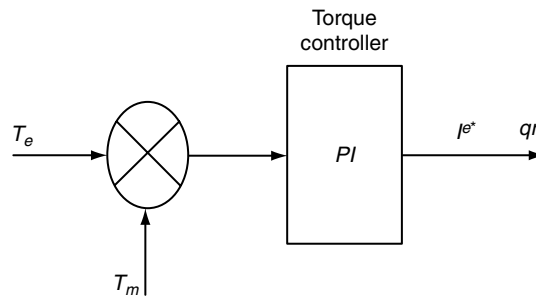


Figure 2: Torque controller.

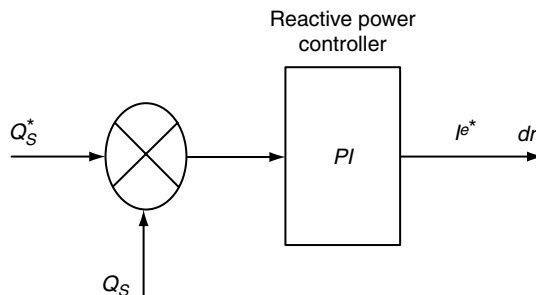


Figure 3: Reactive power controller.

The magnitude of the stator flux linkage and its phase angle are given by:

$$\lambda_s = \sqrt{[(\lambda_{ds}^s)]^2 + [(\lambda_{qs}^s)]^2}$$

$$\theta_e = \tan^{-1} \frac{\lambda_{qs}^s}{\lambda_{ds}^s}$$

$$\therefore \theta_{slip} = \theta_e - \theta_r$$
(10)

During normal operation, GSC principally maintains dc link capacitor voltage constant regardless of the direction and magnitude of the rotor power. As the converters are rated for a small fraction of generator rating, the reactive power reference is set to zero. However, reactive power controllability will be useful during the process of voltage reestablishment for duration while RSC remains blocked after a grid fault has been cleared [17]. The RSC performs independent control of speed/real power, reactive power between DFIG and the grid, by means of rotor current regulation employing two stage controllers. Thus, DFIG can be operated at any desired power factor by injecting small reactive power into the rotor circuit using RSC. These features make DFIG, a versatile electrical machine for grid integration of wind power generation facilities.

3. PROPOSED FRT SCHEME

The structure of proposed FRT scheme, which is connected between the rotor circuit and dc link capacitor in parallel with RSC is shown in Fig. 4. This scheme consists of an uncontrolled rectifier, two sets of IGBT switches S1, S2, diode D and storage inductor L.

3.1. Control strategy of proposed FRT scheme

During normal operation, the IGBT switches S1 and S2 remain open and diode D is reverse biased, therefore the proposed FRT scheme does not interfere the normal operation of DFIG.

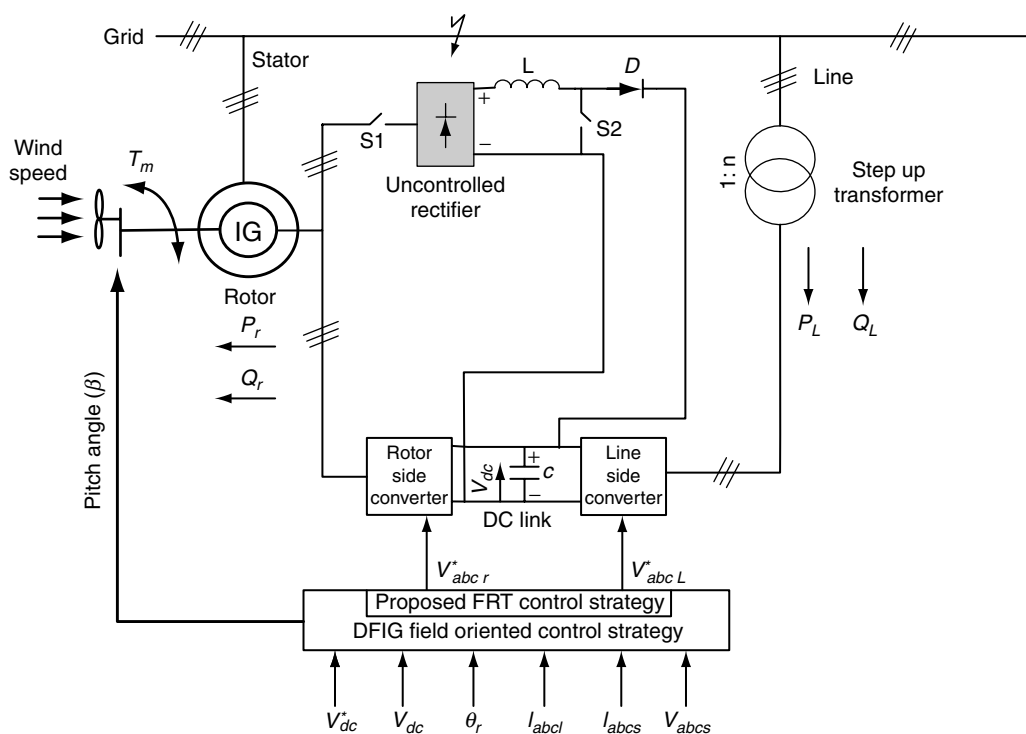
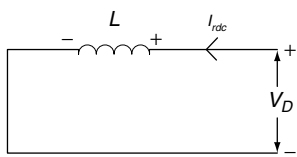
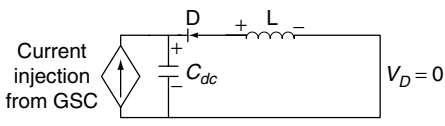


Figure 4: Proposed fault ride-through scheme and control for DFIG.

During grid faults, DFIG terminal voltage drops to a very low value and the stator current rises rapidly. The stator disturbance is further transmitted to the rotor because of magnetic coupling between them. This will result in high transient current in the rotor circuit that may damage the power electronic devices in the rotor converter. In order to protect the converter, gating signals to RSC are blocked whenever the rotor current exceeds the semiconductor device ratings. This increase was avoided by using a de-saturation detection technique [18], provides the state of electrical over stress of IGBT under current fault condition when gate voltage is high. Reducing gate voltage in a controlled manner to just above gate threshold voltage is preferred. This will reduce fault current and after some finite time gate voltage is brought down to zero safely, turning off the IGBT without stress. Though the devices are now protected, the transient current in the rotor circuit now raises the dc link voltage through the anti-parallel diodes of RSC. Therefore, a suitable control technique is proposed in this paper so as to protect the rotor converter against over-current and the dc link capacitor against excessive over-voltage. The mode and sequence of operation of the proposed FRT scheme is shown in Table 1.

In the proposed FRT scheme, when the rotor current is more than the permissible limit, gating signals to RSC are blocked. Simultaneously, the switches S1 and S2 are closed if either the terminal voltage dip is more than the threshold value or the dc link capacitor voltage goes beyond the permissible limit. Since the generator and converter stay connected, the synchronism of operation remains established during and after the fault. Normal operation can be restored immediately after the fault is cleared. As soon as the rotor current decreases below the permissible limit, gating signals to RSC are restored unlike the crowbar

Table 1: Sequence and mode of operation of proposed FRT scheme

On fault occurrence (Mode-1)	On fault clearance (Mode-2)
<ul style="list-style-type: none"> • If the rotor current exceeds the permissible limit, block gating signals to the RSC. • Measure the terminal voltage and compute the voltage dip (ΔV). • If either the voltage dip (ΔV) is more than the threshold value or dc link voltage level exceeds its limit, connect the proposed FRT scheme by closing the switches S1 and S2. • After initial rotor current transients die out, restore gating signals to RSC when the rotor current reduces below the permissible limit. • Input mechanical energy of the wind turbine is stored in inductor L of the proposed FRT scheme through uncontrolled rectifier and switches S1 and S2. 	<ul style="list-style-type: none"> • Measure the terminal voltage and compute the voltage dip (ΔV). • If the voltage dip (ΔV) is less than the threshold value, disconnect the FRT scheme by opening the switches S1 and S2. • The stored electromagnetic energy in the inductor is transferred into the dc link capacitor
 <p>IGBT Switches S1 and S2 are closed</p>	 <p>IGBT Switches S1 and S2 are opened</p>

protection scheme, where the gating signals to RSC are established only after the terminal voltage restores above a certain limit [19]. Thus, generator magnetization is done over the rotor circuit with the help of RSC. Now the input mechanical energy of the wind turbine is stored as electromagnetic energy in the inductor L . Since a torque balance is established between the developed electromagnetic torque of induction machine and the input mechanical torque of the wind turbine, the rotor speed deviation is reduced. Thus the reactive power requirement of DFIG on fault clearance is also reduced in accordance with the reduction in the rotor speed deviation [20] with the help of proposed FRT scheme.

On fault clearing, when the voltage dip is reduced below the threshold value, the switches S1 and S2 are opened. Now the diode D gets forward biased and the stored energy in the inductor L is transferred into the dc link capacitor C_{dc} . Consequently, the GSC current needed for charging the dc link capacitor is reduced and the converters can be used to its full capacity in restoring the normal operation of DFIG.

3.2. Choice of size of storage inductor

The selection of the size of inductor L in the proposed FRT scheme is similar to that of the crowbar resistance scheme. Small value of crowbar resistance (R_{cw}) does not limit the rotor current and cause torque transient peaks during the fault moment. Higher R_{cw} has an efficient damping effect on the rotor current and electromagnetic torque. It also reduces the reactive power requirement at the instant of fault clearing. However, a very high value of R_{cw} can imply a risk of excessive transients in rotor current, torque and reactive power while removing the crowbar [21]. Similarly, if the inductor size is too small, the entire mechanical energy of the wind turbine during the transient period cannot be stored. Large inductor size will make the scheme bulky and costly. Considering the correct choice of R_{cw} obtained for an existing DFIG machine, a procedure is presented in this section to acquire an initial guess for the choice of storage inductor L .

In the proposed FRT scheme, in order to achieve a performance equivalent to that of the active crowbar scheme, the energy content of the storage inductor should be at least equal to the energy dissipation capacity of the crowbar resistor R_{cw} in active crowbar scheme. With this hypothesis, the size of storage inductor is computed as follows.

Neglecting switching losses in the power electronic devices, the energy dissipated in the resistor R_{cw} of an active crowbar FRT scheme during the fault event is given by

$$E_{cw} = I_{rdc}^2 R_{cw} t_f \quad (11)$$

Where I_{rdc} is the Rectified Rotor current (A); R_{cw} , the Crowbar resistance (Ω) and t_f is the Fault duration (s).

During same fault duration, the energy required to be stored in inductor L , employing the proposed FRT scheme is given by

$$E_L = \frac{1}{2} I_{rdc}^2 L \quad (12)$$

Where L is storage inductance in (H).

Based on the hypothesis, the capacity of energy content of the inductor should be greater than or at least equal to the dissipation capacity of the resistors R_{cw} in the crowbar FRT scheme, i.e.

$$E_L \geq E_{cw} \quad (13)$$

Thus, from (11)–(13),

$$\frac{1}{2} i_{rdc}^2 L \geq i_{rdc}^2 R_{CW} t_f \quad (14)$$

From (14), the choice of inductor size is computed as,

$$L \geq 2 R_{CW} t_f \quad (15)$$

Equation (15) is a good starting point for selection of the inductor size in the proposed FRT scheme.

4. SIMULATION STUDY

The detailed simulation study and performance evaluation of the proposed FRT scheme have been dealt in this section. A 9 MW DFIG machine connected to weak power system network is simulated using MATLAB/SIMULINK software. The machine parameters are given in the Appendix [A]. Single line to ground fault is simulated at 2s and sustained for a period of 500 ms, a duration during which the wind turbine is required to remain connected and operational as per grid code requirement. Owing to large mechanical time constant of wind turbine, the variations in wind speed during the fault event is ignored. The performance of the proposed FRT scheme for a severe symmetrical grid fault condition, where the terminal voltage goes down to zero volts, is compared with that one of rotor short circuited.

The proposed one is expected to perform as ZVRT scheme. The crowbar resistance ($R_{\downarrow cw}$) is chosen as 1.486Ω ($R_{\downarrow cw} = 20 R_r$), where R_r is the rotor resistance as recommended in [20] and utilized in [22]. As wind generators are expected to be disconnected from the grid for fault duration longer than $t_f = 0.5s$ [7, 8], the size of the inductor utilized in the proposed scheme is computed as follows:

$$R_{CW} = 20 R_r; t_f = 0.5 s; \text{ Using (15) }, L \geq 2 R_{CW} t_f; L \geq 0.38 H.$$

Therefore, an inductor of $L = 0.5 H$ is chosen for the simulation study.

Using crowbar protection scheme, the input mechanical energy from the wind turbine is dissipated as heat in the crowbar circuit during the fault period. Hence, this method needs to confront the troublesome evacuation of heat generated in the resistors of the crowbar circuit during severe faults [22]. Therefore, an attempt is made in this paper employing a simple additional circuitry instead of resistor crowbar circuit to temporarily store the input mechanical energy of the wind turbine during the fault period and subsequently utilize the same for charging of DC link capacitor on fault clearance.

The sequence of operation of the proposed FRT scheme is discussed in Section 3. In response to grid fault, terminal voltage decreases and currents in the stator and rotor circuit increases rapidly, this can be shown in figures 4.1.5, 4.1.6, 4.1.7, 4.1.8, 4.1.9, 4.1.10, 4.1.11, 4.1.12 and 4.1.13. As the rotor current exceeds the permissible limit, the gating signals to RSC are blocked. Since the dip in terminal voltage has already surpassed more than the threshold value, switches S1 and S2 are turned ON and the proposed FRT circuit gets connected to the rotor circuit. Since the FRT circuit is connected, the rotor current subsides below the permissible limit and the gating signals to RSC are restored and generator magnetization is done over the rotor circuit. Now the input mechanical energy of the wind turbine gets stored as electromagnetic energy in the inductor L , instead of being dissipated

in the resistor R_{cw} as in the case of an active crowbar. Since the torque balance is achieved between the developed electromagnetic torque of induction machine and the input mechanical torque of the wind turbine as illustrated in figure 4.2.15, the mechanical torque and so rotor speed are nearly maintained at the pre-fault value as shown in figure 4.2.14 if it is compared with that one in case of rotor short circuited during fault as shown in figure 4.1.14.

Consequently the reactive power requirement of DFIG on fault clearance shown in figure 4.2.3 is also greatly reduced due to large reduction in rotor speed deviation from its pre-fault value. Hence rapid recovery of terminal voltage of DFIG to nominal voltage, which can be inferred from voltages waveforms, is accomplished with the help of proposed FRT scheme; this is illustrated in figures 4.2.5, 4.2.6 and 4.2.7. Also it is clear that the fluctuations in electromagnetic torque and powers of DFIG at the instant of fault clearing are also greatly reduced as shown in figures 4.2.2 and 4.2.14.

On fault clearing, when the dip in terminal voltage is still below the threshold value, the switches S1 and S2 are turned OFF. Now the diode D gets forward biased and the stored energy in the inductor L is transferred into the dc link capacitor C_{dc} , charging it to 1.03 p.u momentarily for a short duration, however it reduces back to its reference value at 2.6 s, this is viewed through figure 4.2.4. Consequently, the current in GSC needed for charging the dc link capacitor is also reduced and thus the proposed FRT scheme assists GSC and RSC in restoring the normal operation of DFIG as shown in figures 4.2.8, 4.2.9, 4.2.10, 4.2.11, 4.2.12 and 4.2.13, which show the reduction in line and rotor currents after using the proposed scheme. In this scheme, it is observed that the performance of DFIG has improved to a greater extent and comply with the grid code requirements.

A Three phase to ground fault was applied across the grid terminals at $t = 2$ s for 500 ms duration. The performance of the wind generation system under the fault can be observed through figure 4.3, which illustrates that the terminal voltages were dropped to very low values as viewed in figure 4.3.4. The generator tends to absorb a large amount of reactive power during fault this can be viewed in figure 4.3.3, which induces instability in the grid, makes high fluctuation in the active power and line currents which consequently affects the rotor current behavior and the electromagnetic torque of the generator. This can be observed in figure 4.3.2 that shows a severe drop in active power, and figures 4.3.8, 4.3.9, 4.3.10 which illustrate the increase in rotor currents during fault. The effect of three phase fault on DFIG's performance can be also investigated through the increase in dc link voltage and severe reduction in both mechanical and electromagnetic torques; this can be shown in figures 4.3.5, 4.3.6 and 4.3.7 respectively.

After applying the proposed scheme the normal operation of DFIG was restored and the measured values of generated active and reactive power eventually returned to their normal range, this can be shown in figures 4.4.2 and 4.4.3. Figure 4.4.4 shows the positive effect of proposed scheme on the value of dc link voltage during fault period. The reduction in rotor currents to their normal values can also be viewed in figures 4.4.7, 4.4.8 and 4.4.9. Both mechanical and electromagnetic torques were obviously affected by applying the scheme, this can be shown through the restoration of their normal values as viewed in figures 4.4.5 and 4.4.6 respectively.

Based on the results of the parameters of DFIG (namely, electromagnetic torque, reactive power and speed) obtained with the proposed FRT scheme, it can be confirmed that the size of inductor chosen in the present study is more appropriate and thus the proposed method of computation of initial guess for the size of storage inductor is also validated.

4.1. Results during single line to ground fault with short circuited rotor

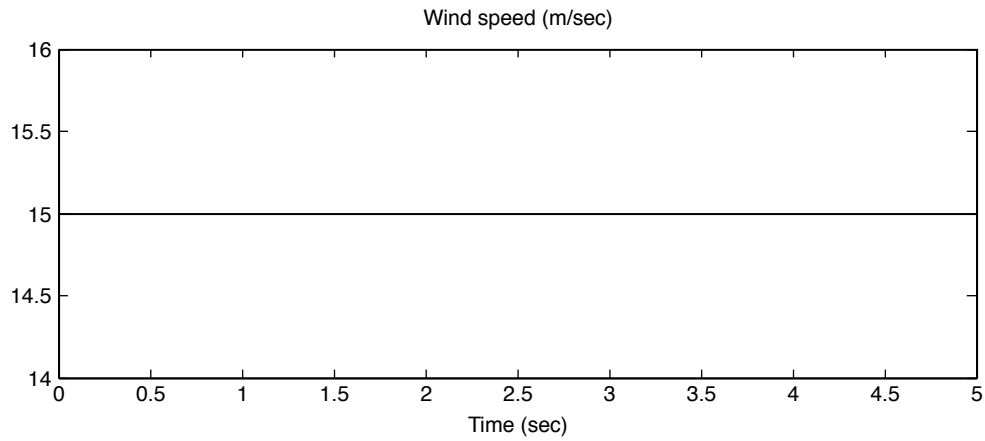


Figure 4.1.1: Wind speed (m/sec).

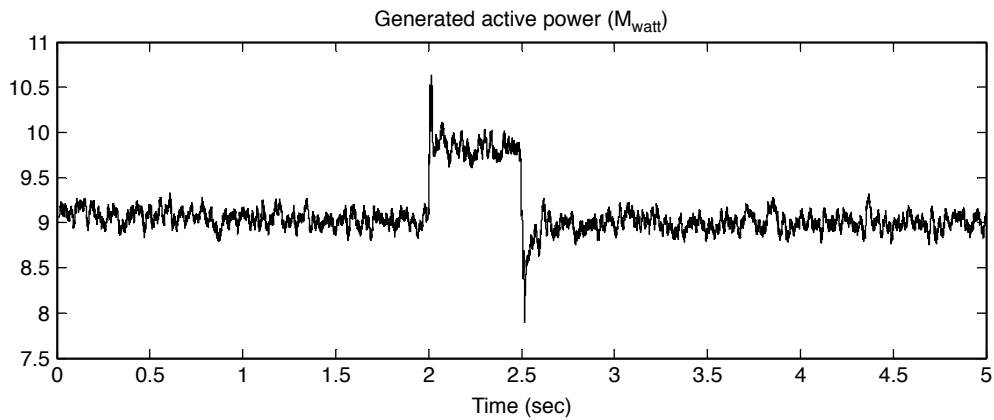


Figure 4.1.2: Generated active power (Mwatt).

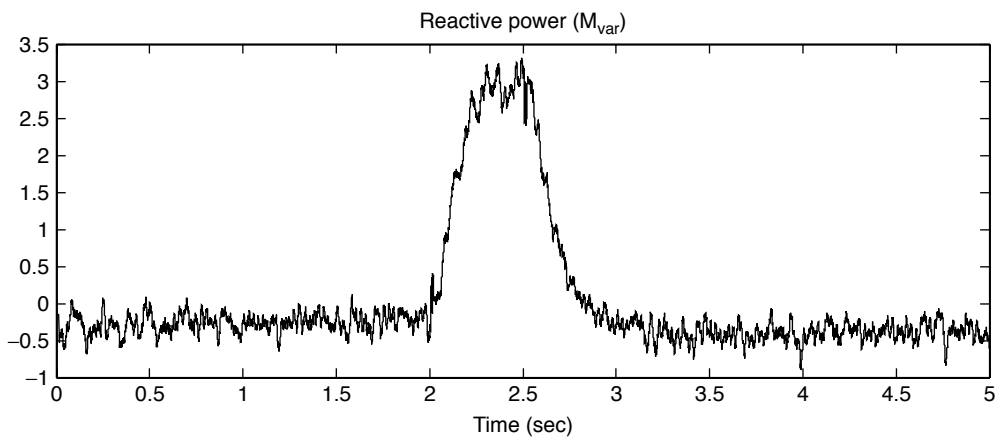


Figure 4.1.3: Generated Reactive power (Mvar).

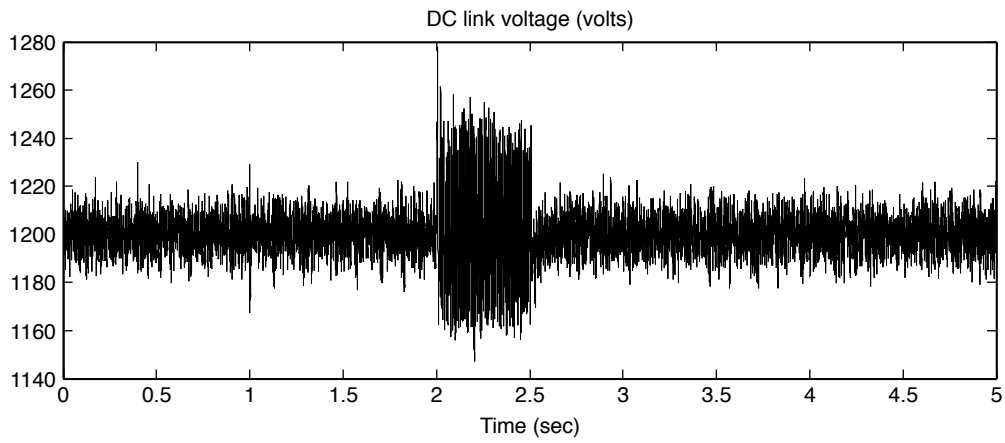


Figure 4.1.4: DC link voltage (Volts).

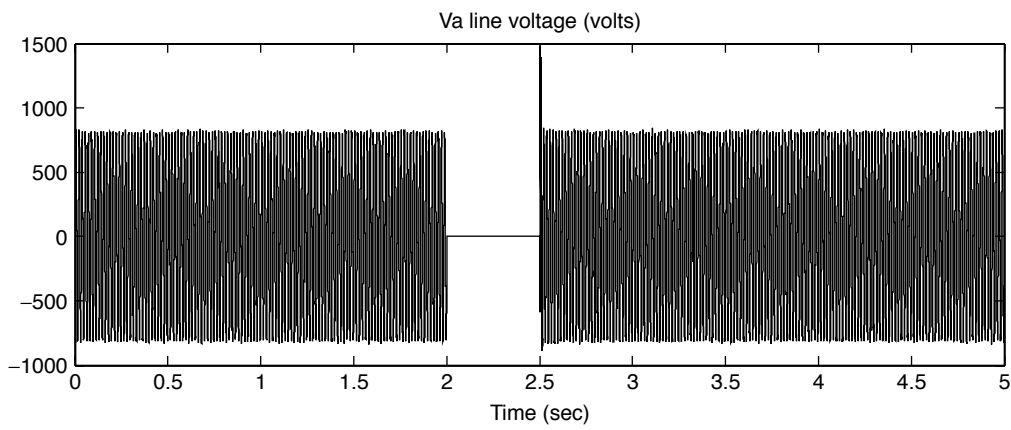


Figure 4.1.5: Phase A line voltage (Volts).

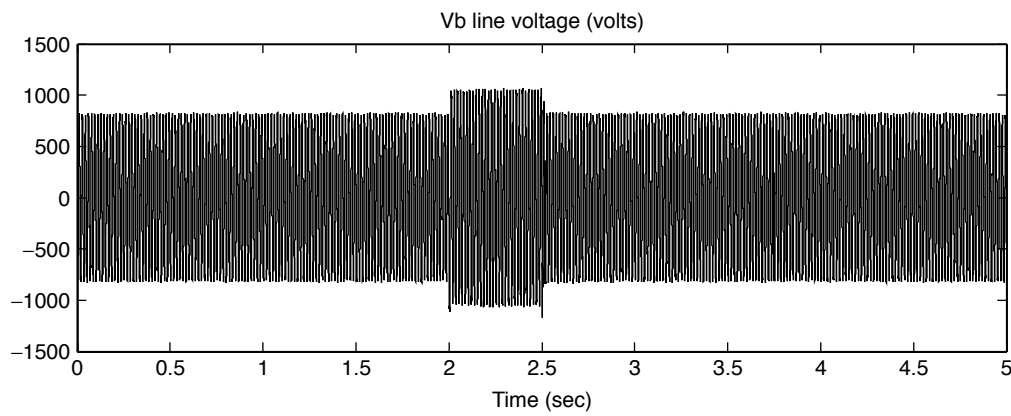


Figure 4.1.6: Phase B line voltage (Volts).

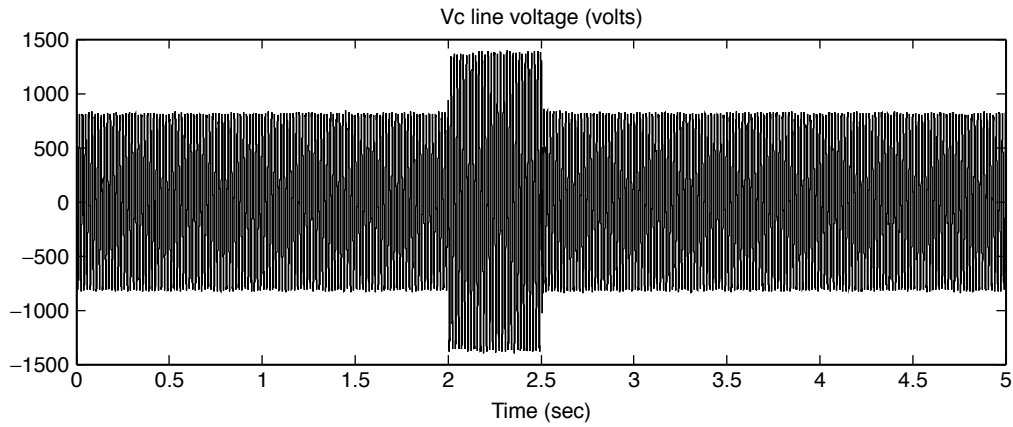


Figure 4.1.7: Phase C line voltage (Volts).

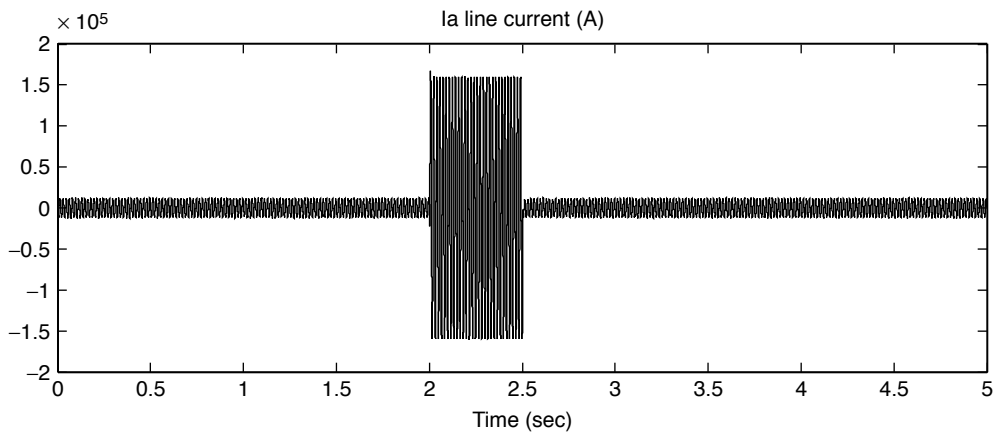


Figure 4.1.8: Phase A line current (A).

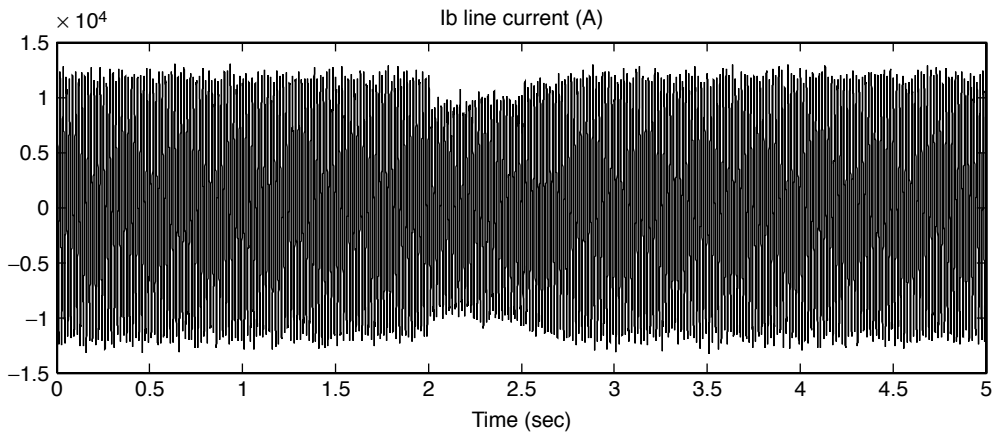


Figure 4.1.9: Phase B line current (A).

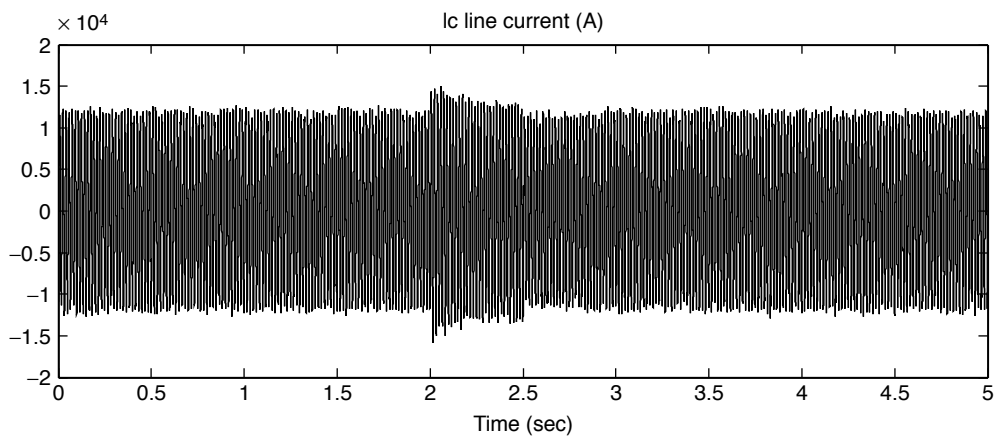


Figure 4.1.10: Phase C line current (A).

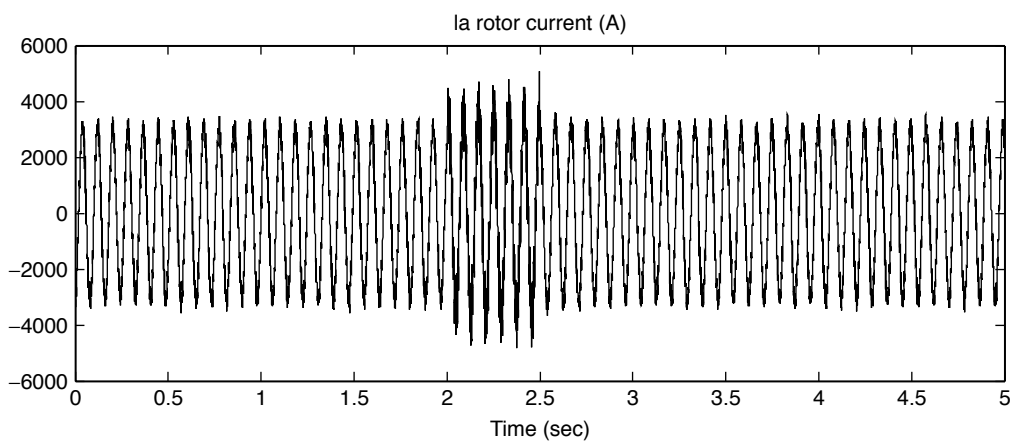


Figure 4.1.11: Phase A rotor current (A).

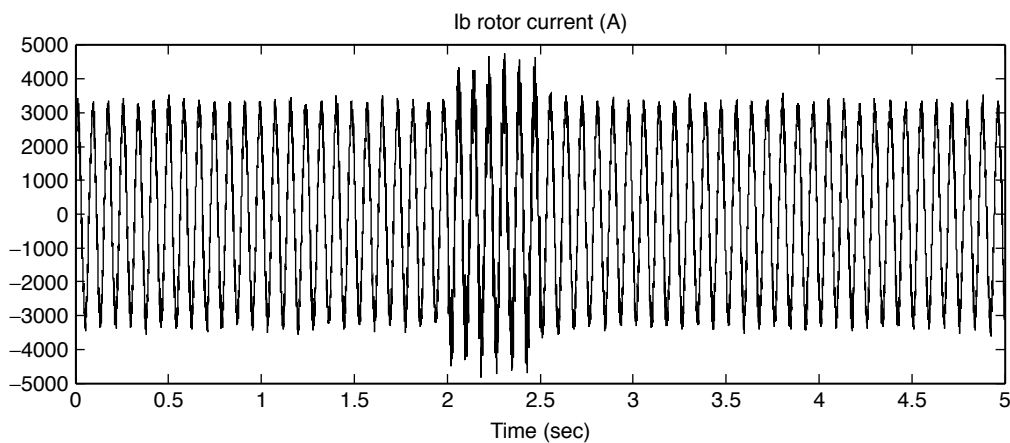


Figure 4.1.12: Phase B rotor current (A).

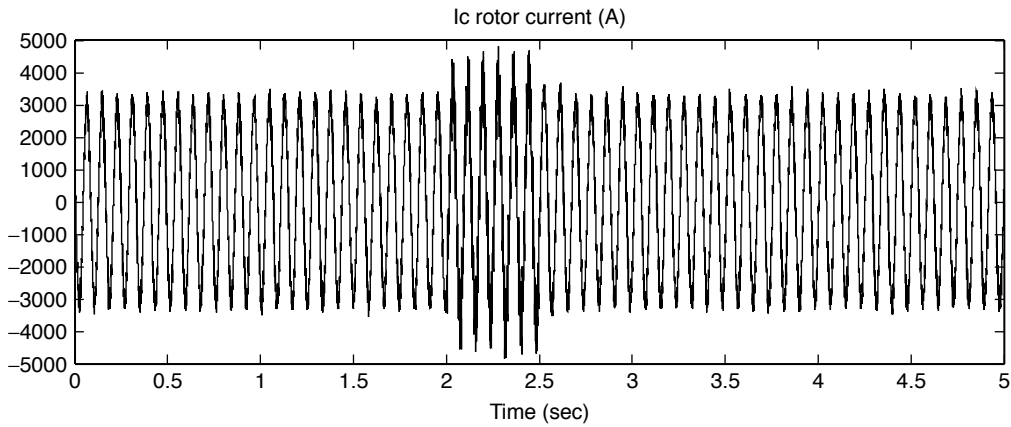


Figure 4.1.13: Phase C rotor current (A).

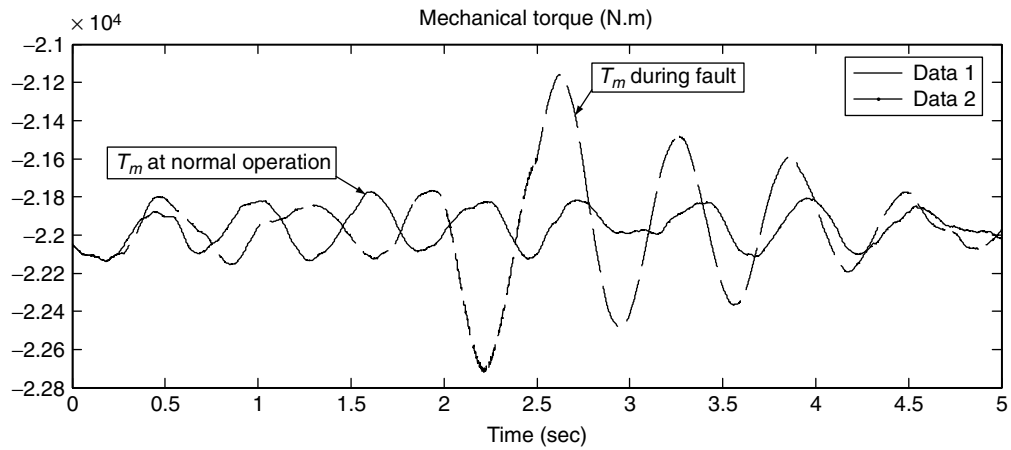


Figure 4.1.14: Mechanical torque (N.m).

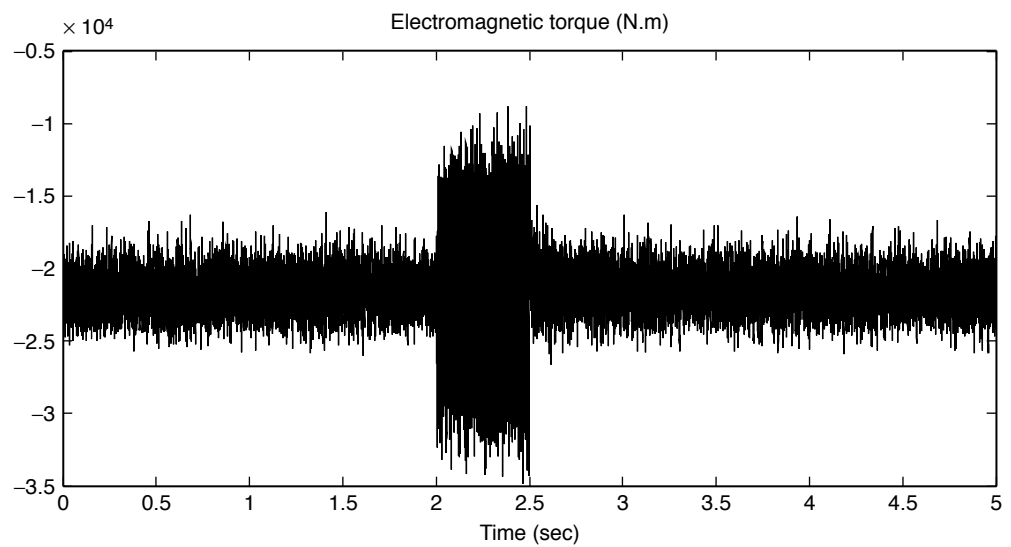


Figure 4.1.15: Electromagnetic torque (N.m).

4.2. Results after using the proposed FRT scheme

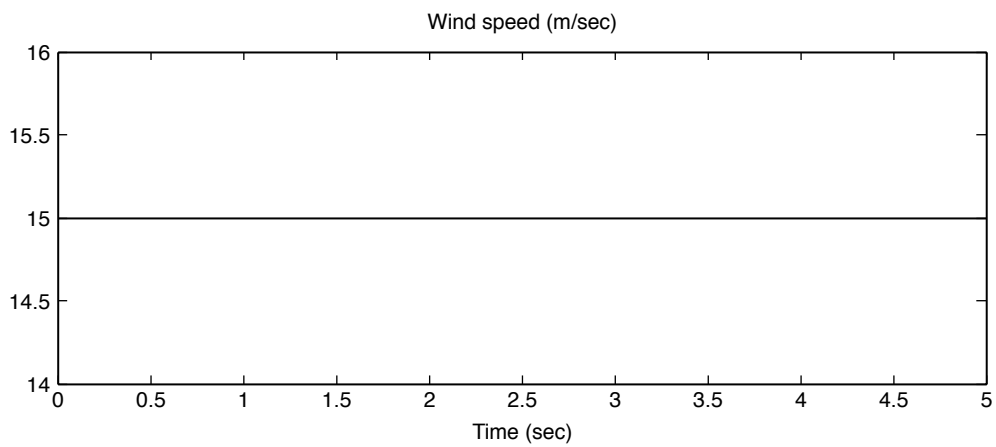


Figure 4.2.1: Wind speed (m/sec).

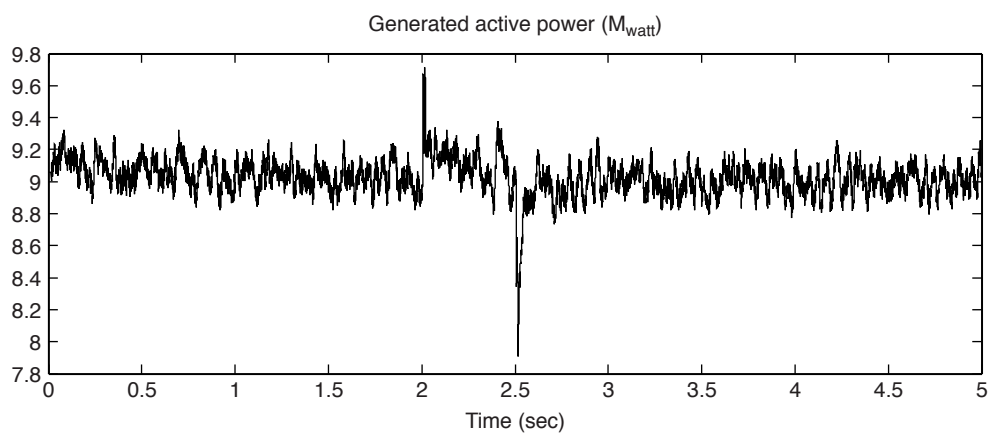


Figure 4.2.2: Generated active power (Mwatt).

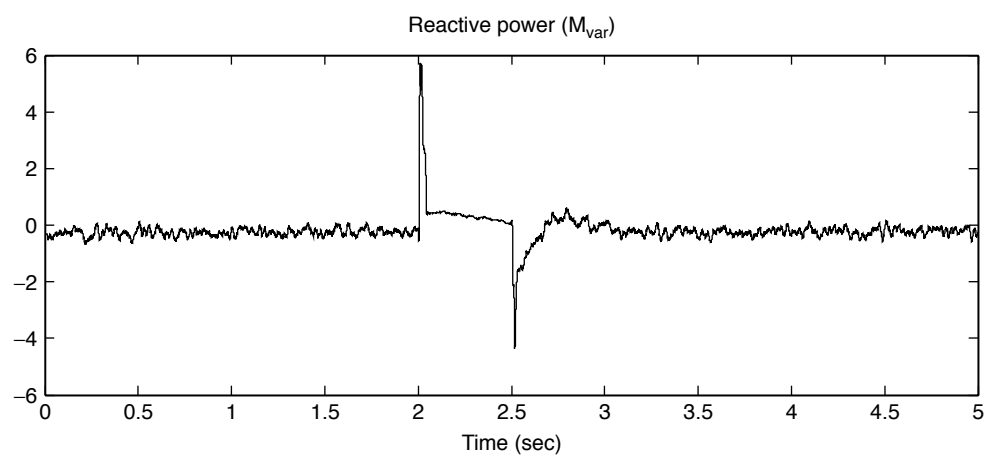


Figure 4.2.3: Generated reactive power (Mvar).

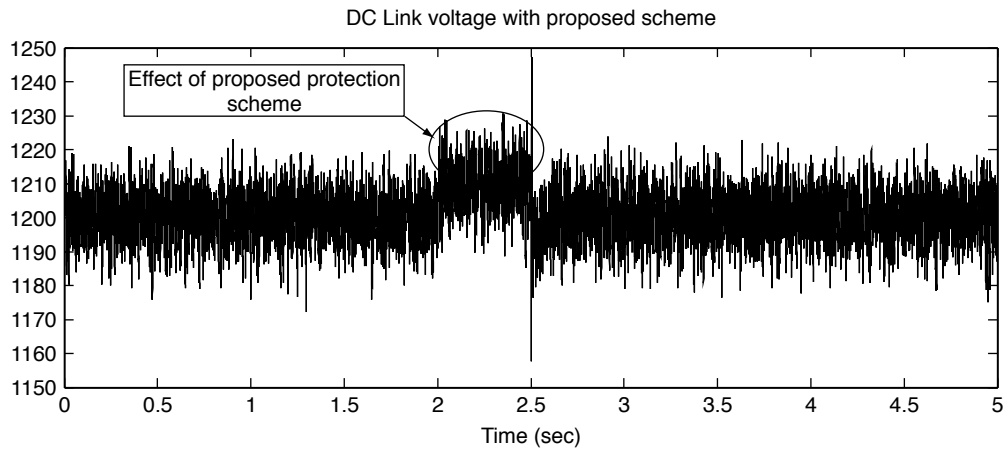


Figure 4.2.4: DC link voltage (Volts).

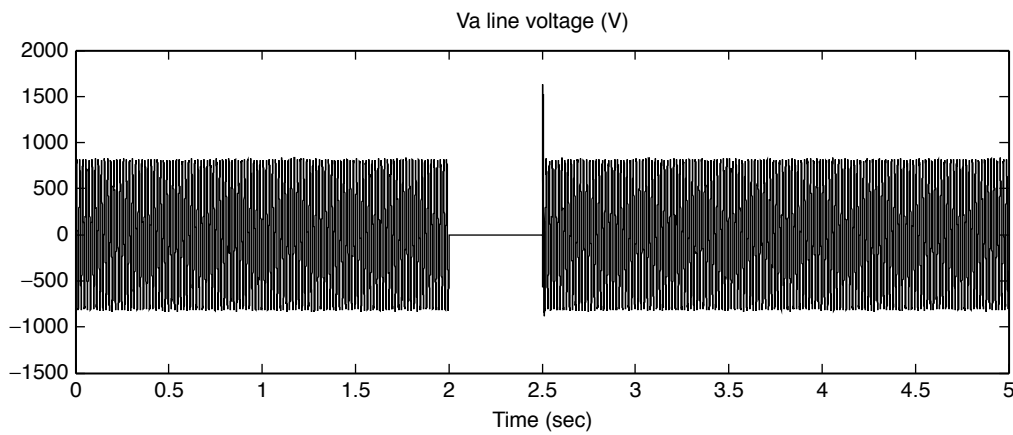


Figure 4.2.5: Phase A line voltage (Volts).

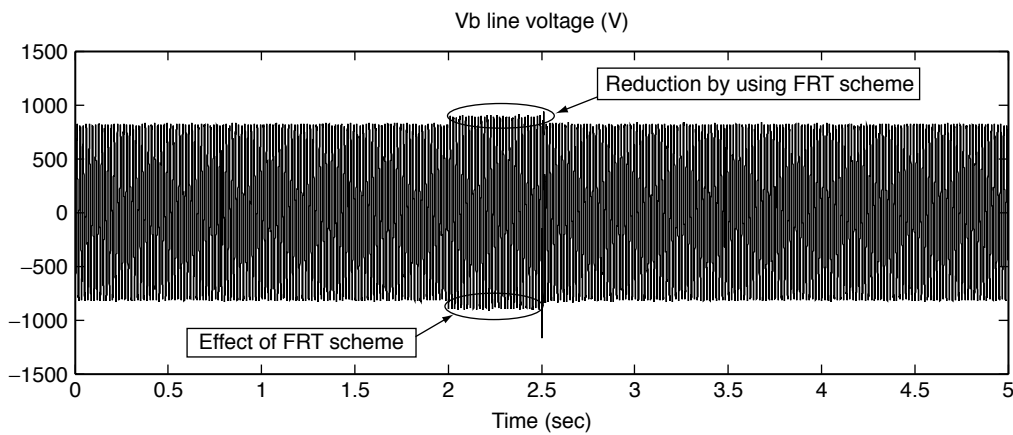


Figure 4.2.6: Phase B line voltage (Volts).

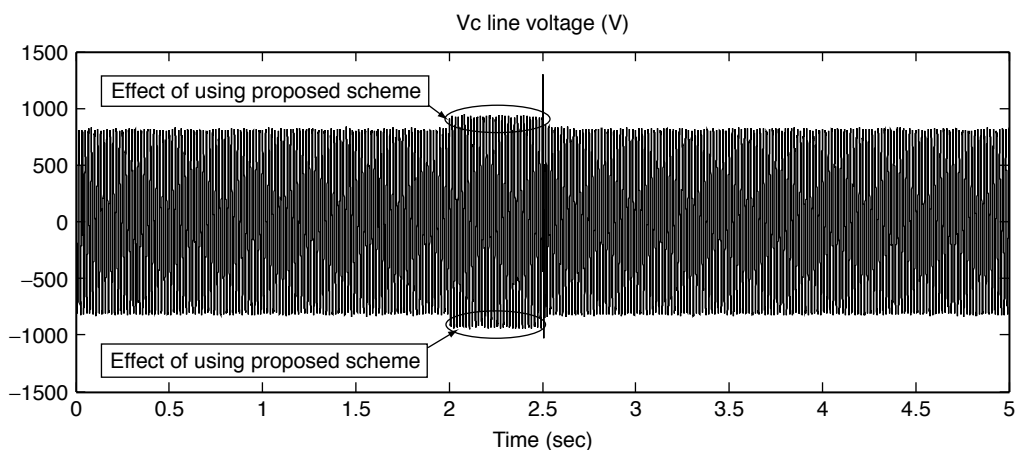


Figure 4.2.7: Phase C line voltage (Volts).

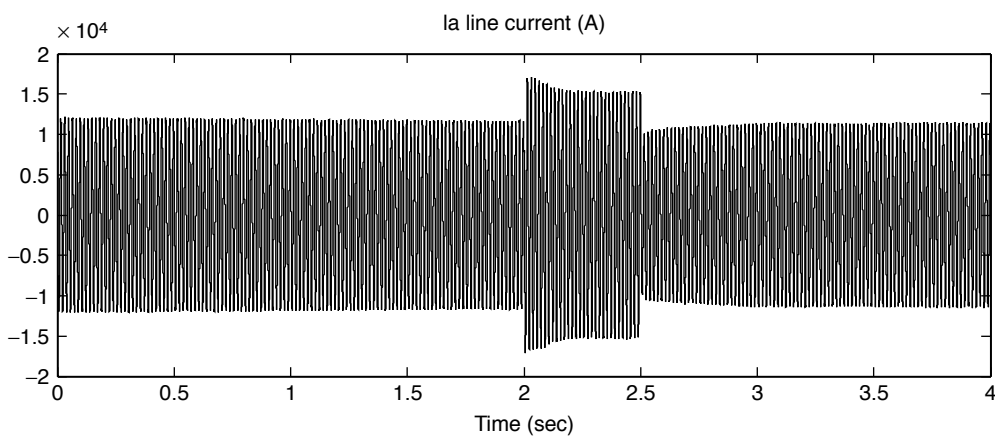


Figure 4.2.8: Phase A line current (A).

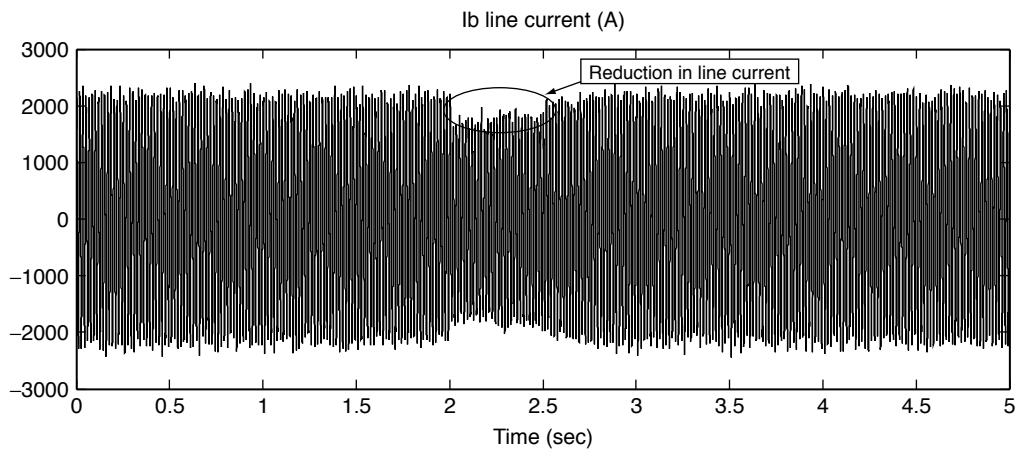


Figure 4.2.9: Phase B line current (A).

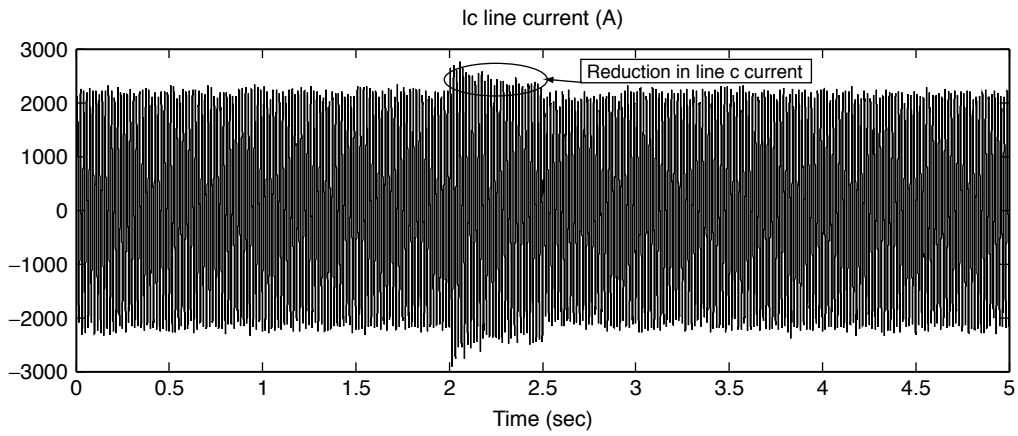


Figure 4.2.10: Phase C line current (A).

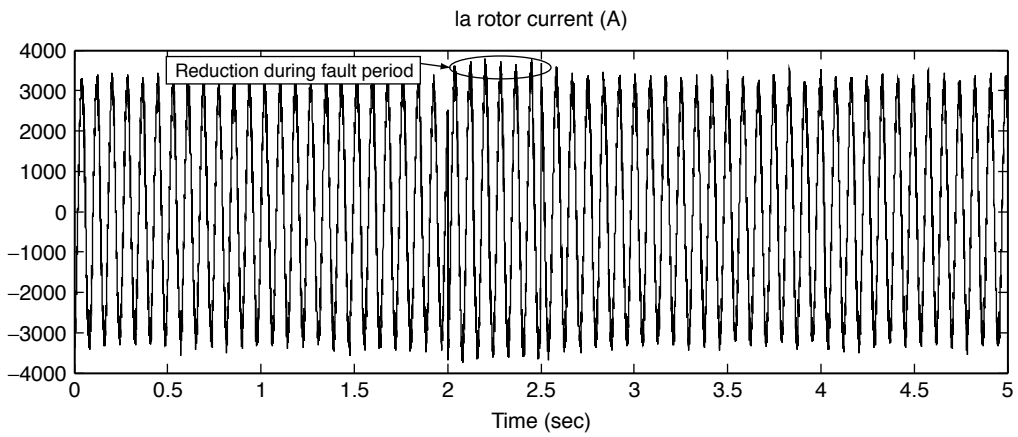


Figure 4.2.11: Phase A rotor current (A).

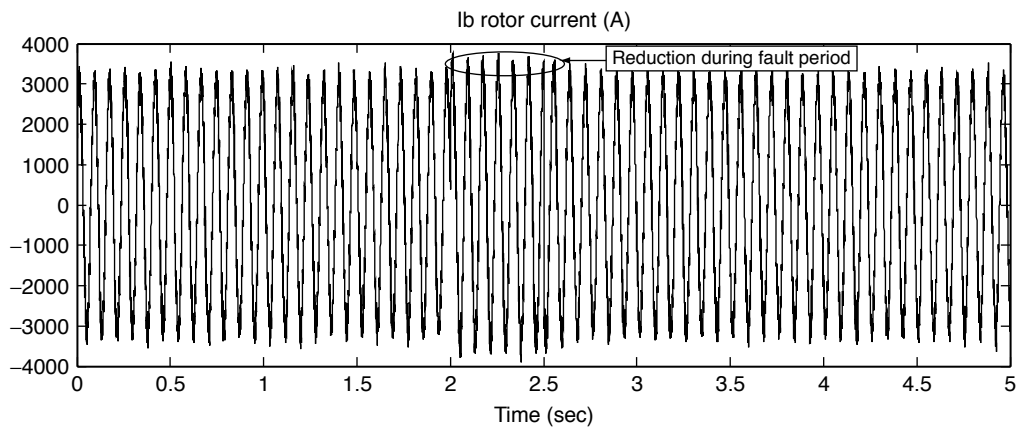


Figure 4.2.12: Phase B rotor current (A).

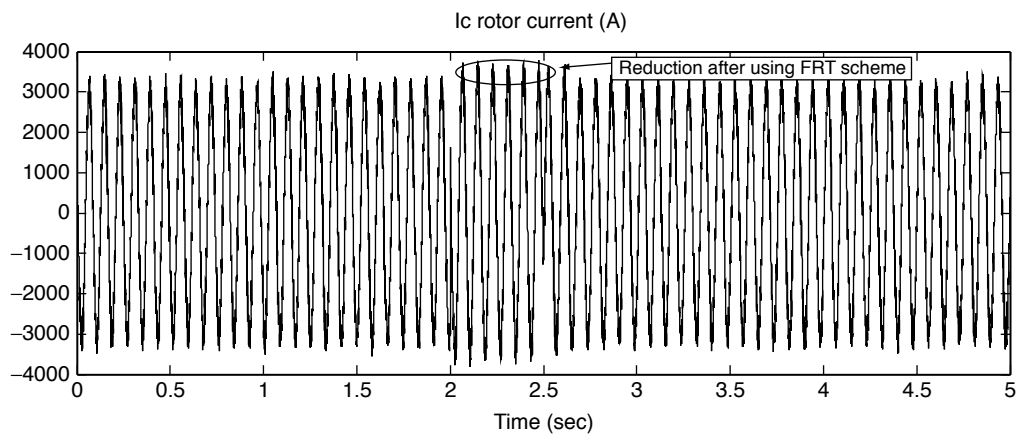


Figure 4.2.13: Phase C rotor current (A).

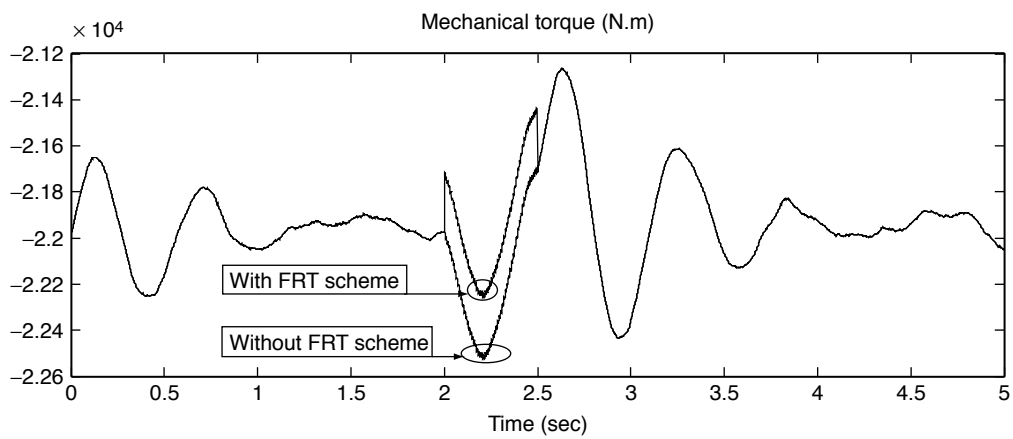


Figure 4.2.14: Mechanical torque (N.m).

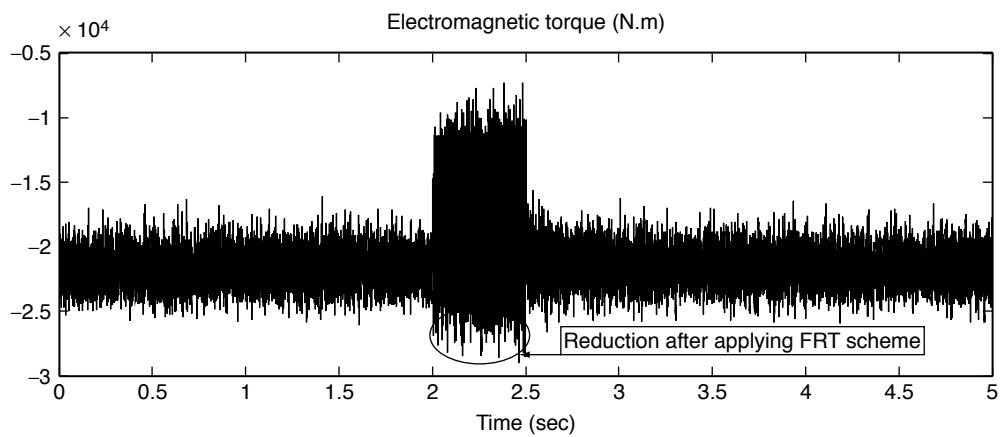


Figure 4.2.15: Electromagnetic torque (N.m).

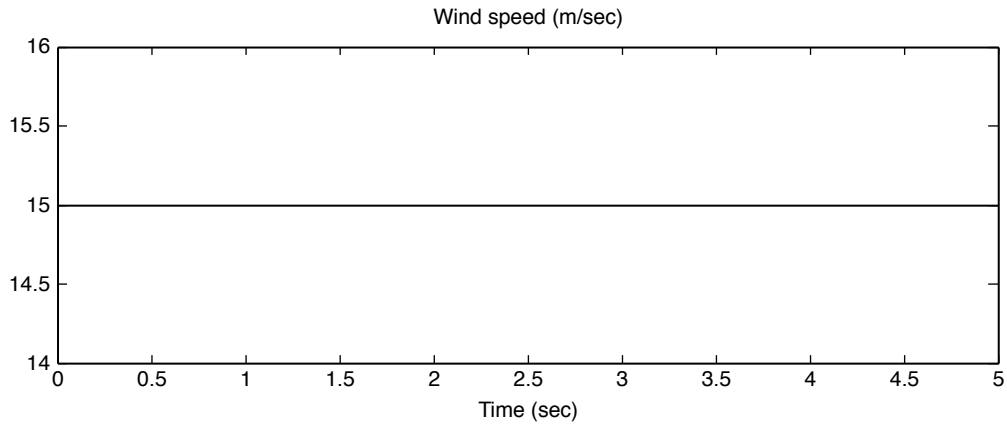
4.3. Results during three phase to ground fault with short circuited rotor

Figure 4.3.1: Wind speed (m/sec).

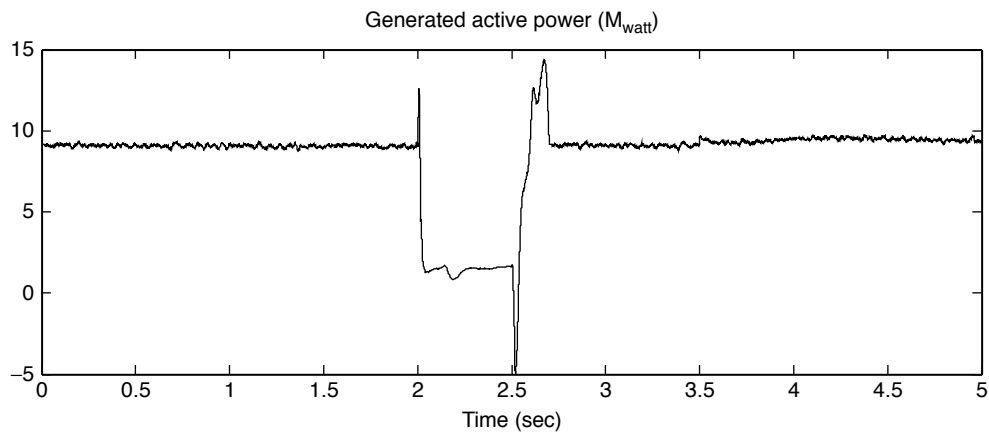


Figure 4.3.2: Generated active power (Mwatt).

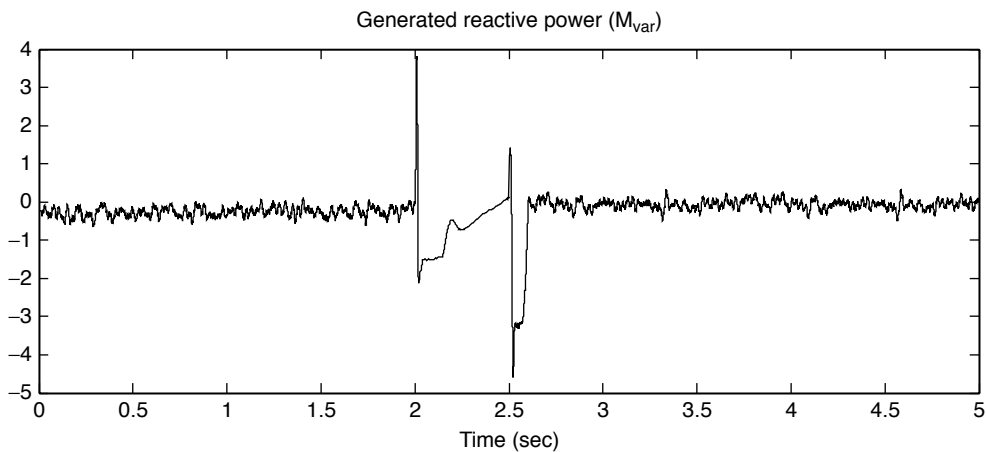


Figure 4.3.3: Generated reactive power (Mvar).

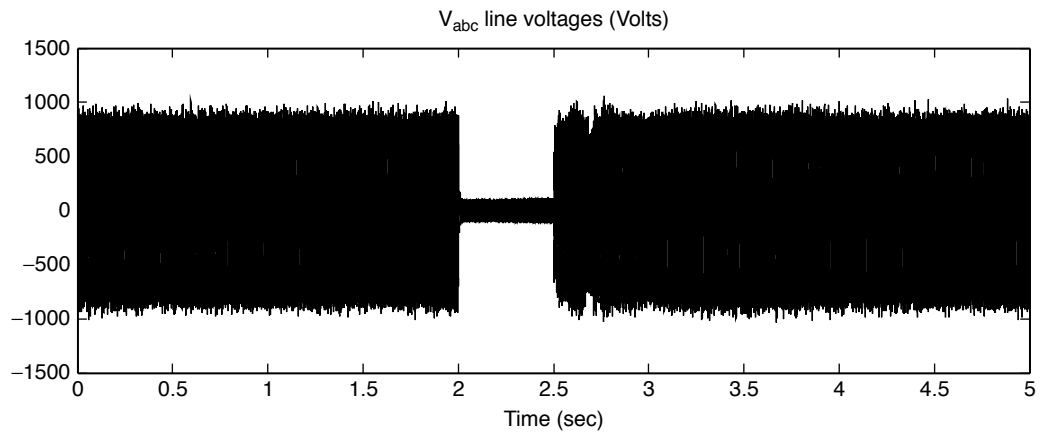


Figure 4.3.4: Three phase line voltages (Volts).

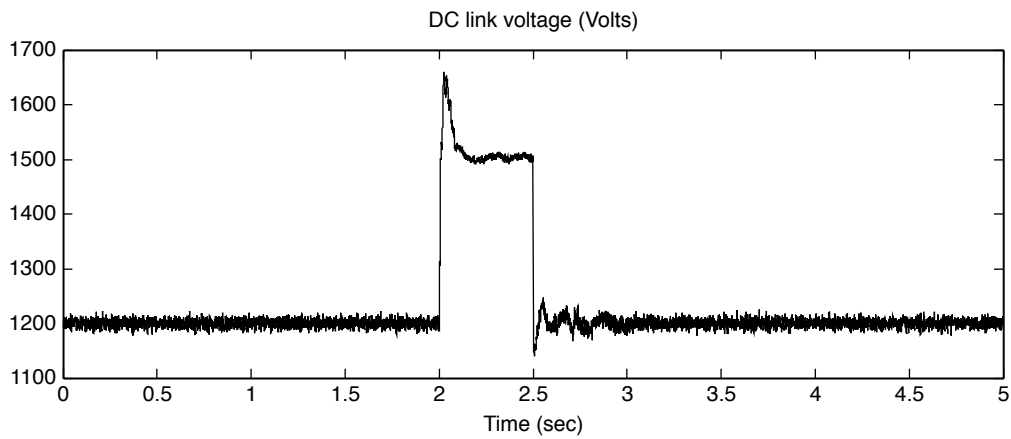


Figure 4.3.5: DC link voltage (Volts).

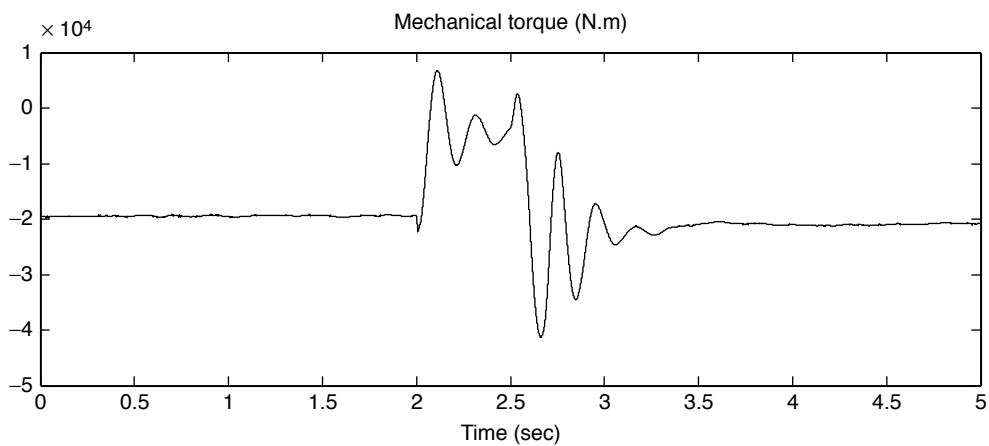


Figure 4.3.6: Mechanical torque (N.m).

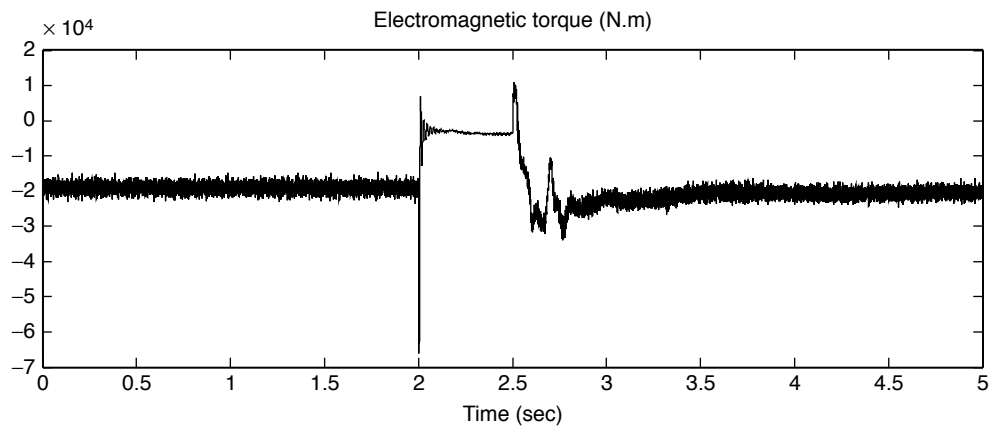


Figure 4.3.7: Electromagnetic torque (N.m).

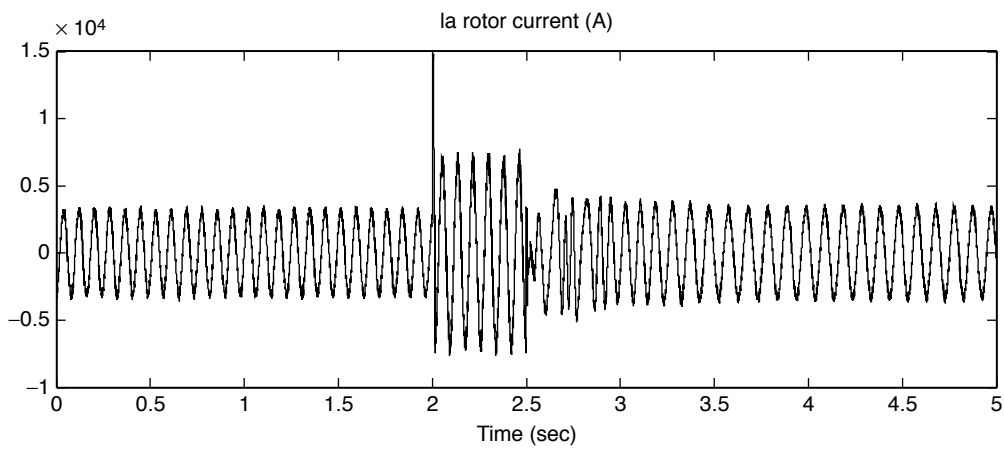


Figure 4.3.8: Phase A rotor current (A).

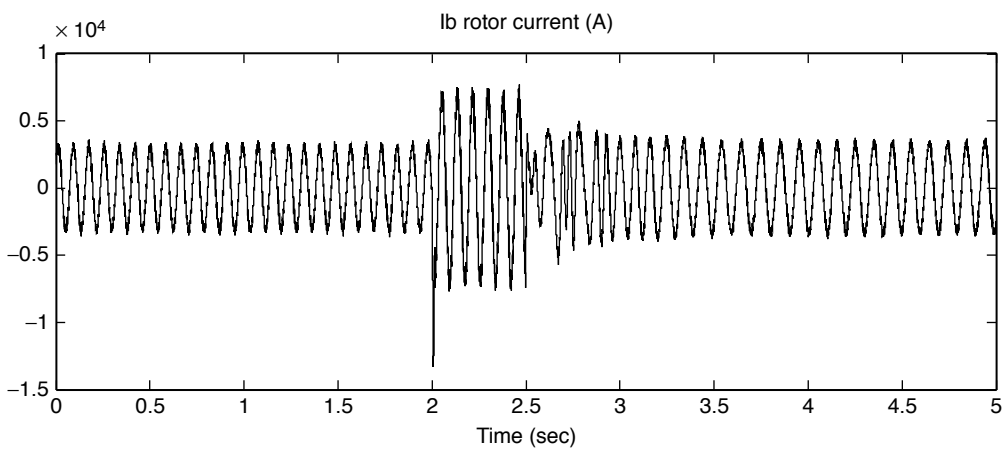


Figure 4.3.9: Phase B rotor current (A).

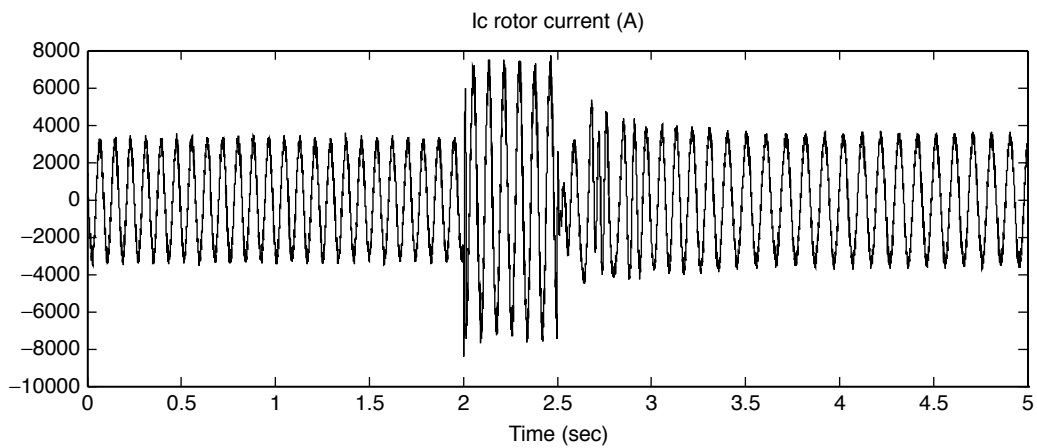


Figure 4.3.10: Phase C rotor current (A).

4.4. Results after using the proposed FRT scheme

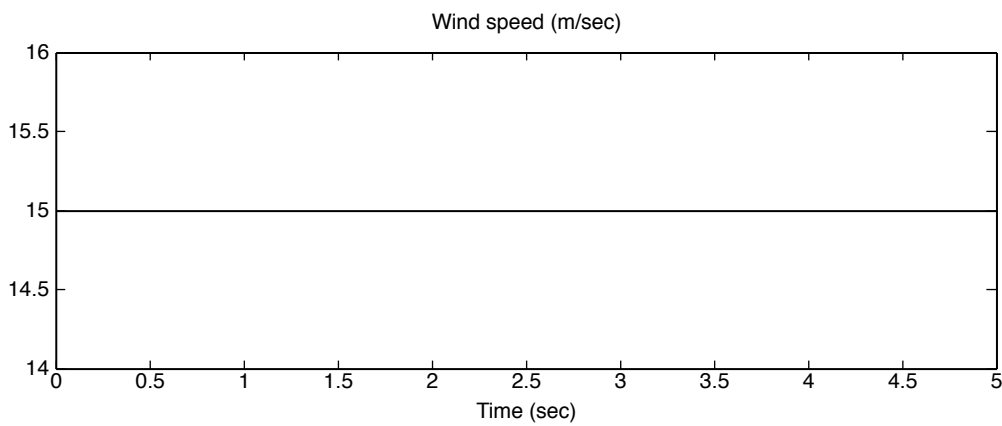


Figure 4.4.1: Wind speed (m/sec).

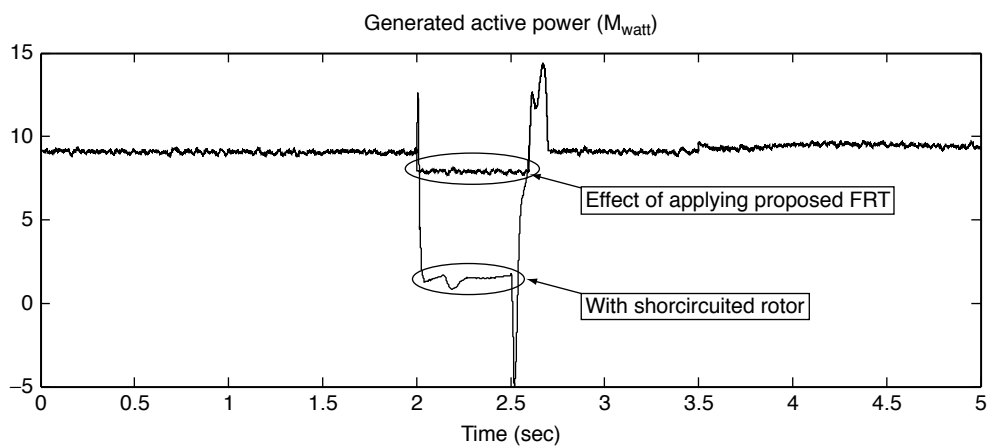


Figure 4.4.2: Generated active power (Mwatt).

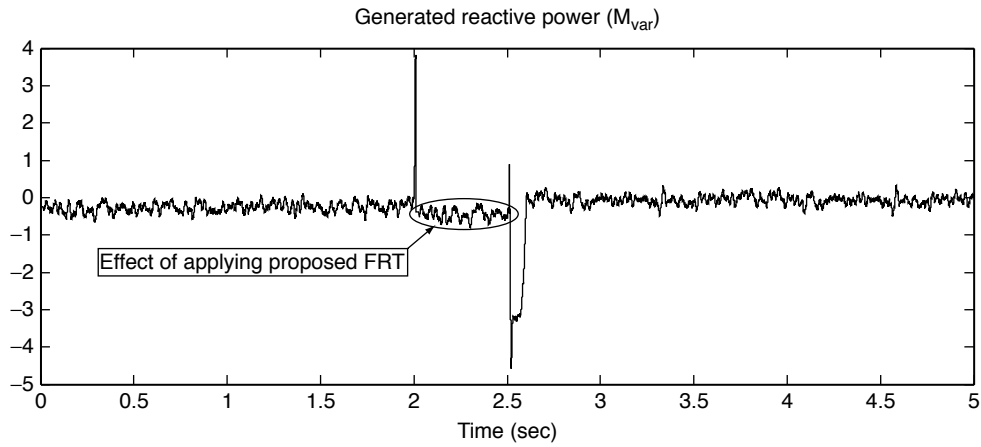


Figure 4.4.3: Generated reactive power (Mvar).

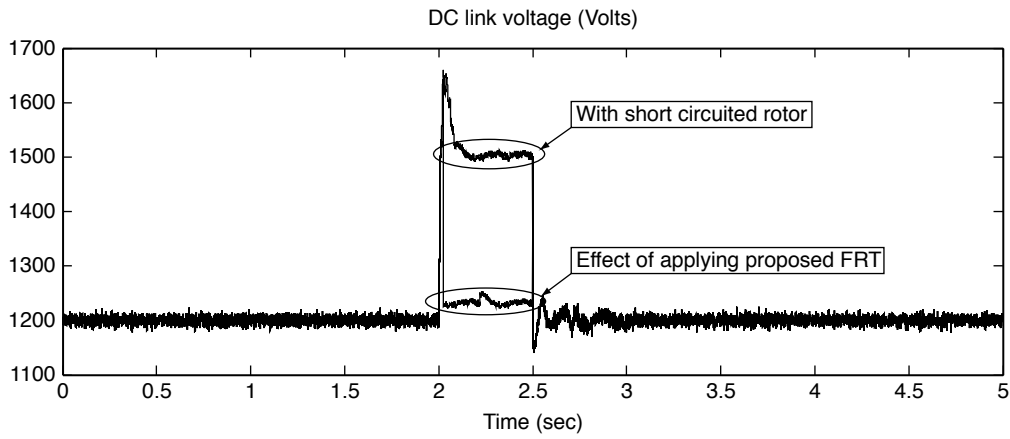


Figure 4.4.4: DC link voltage (Volts).

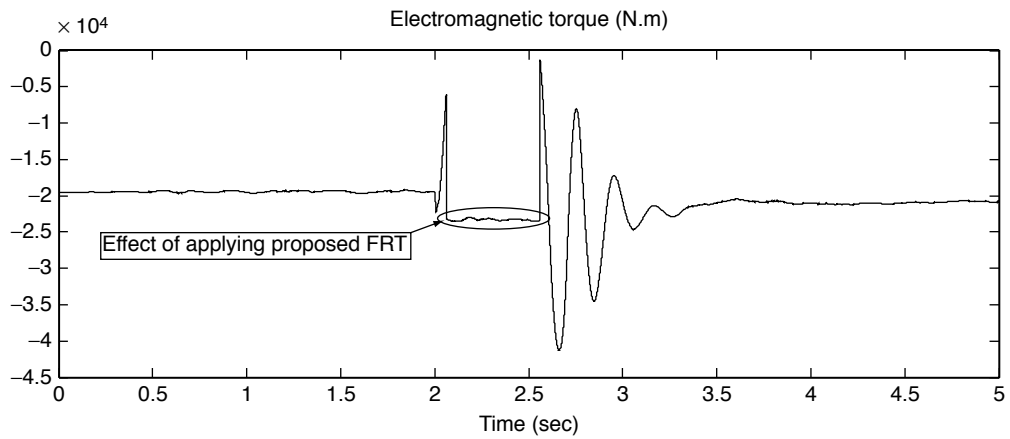


Figure 4.4.5: Mechanical torque (N.m).

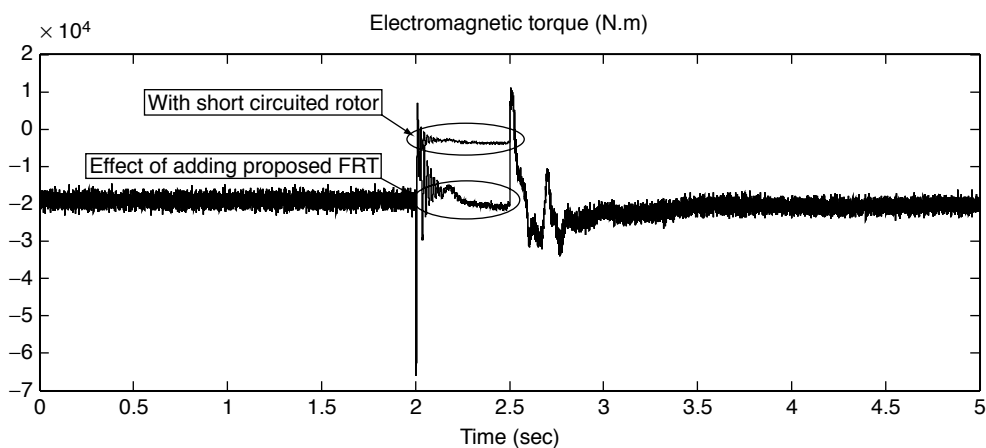


Figure 4.4.6: Electromagnetic torque (N.m).

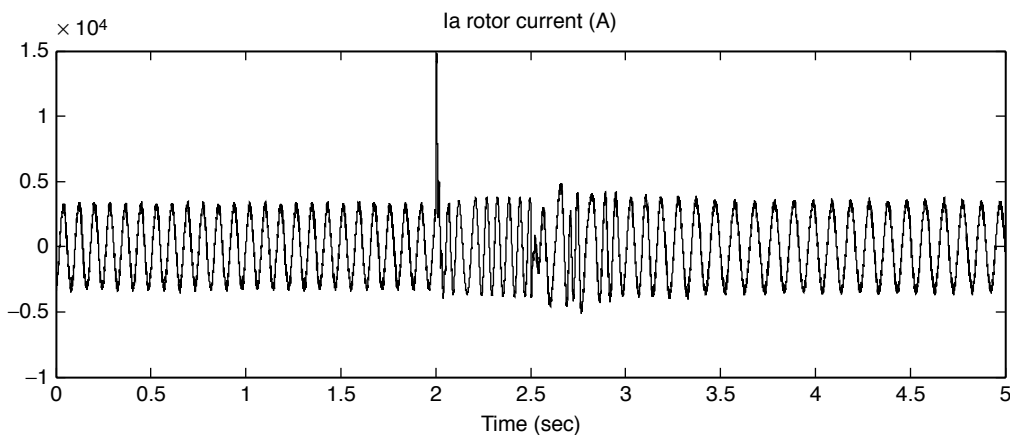


Figure 4.4.7: Phase A rotor current (A).

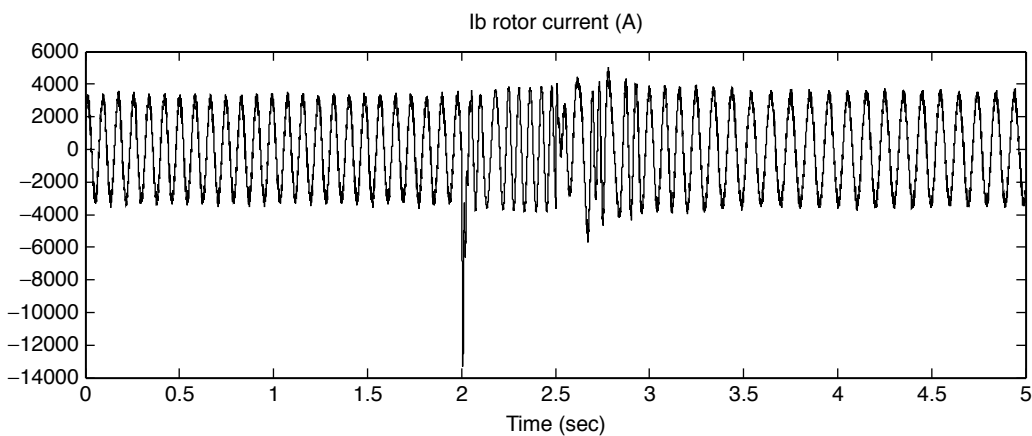


Figure 4.4.8: Phase B rotor current (A).

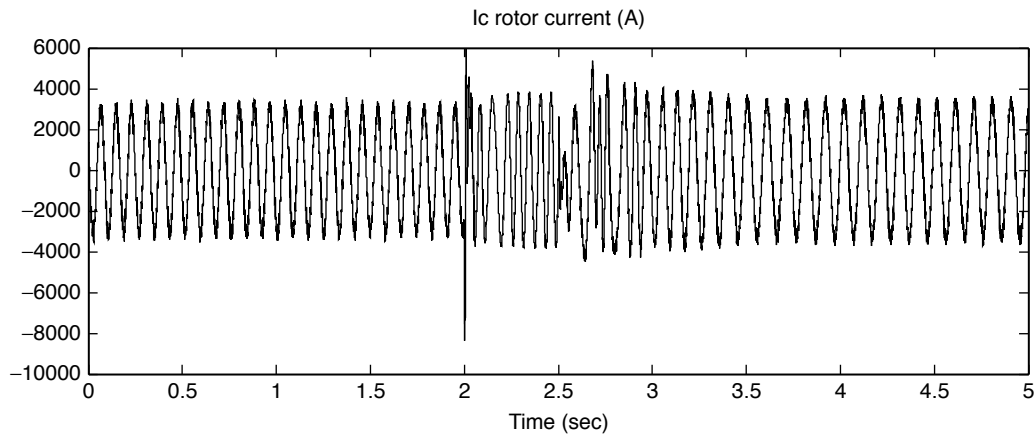


Figure 4.4.9: Phase C rotor current (A).

5. CONCLUSION

A novel fault ride-through (FRT) scheme for doubly fed induction generator (DFIG) based wind farm for achieving enhanced performance capabilities in addition to retaining the generator to stay connected to the power system during grid faults is proposed in this paper. The performance of proposed FRT scheme, which uses minimal additional hardware components rated for rotor circuit power rating, is validated for a severe symmetrical grid fault conditions at the terminal of DFIG. Extensive simulation studies employing MATLAB/SIMULINK software is carried out and the performance of the proposed scheme is compared with other existing FRT schemes namely short-circuited rotor scheme.

In this scheme, the input mechanical energy of the wind turbine during grid fault is stored and utilized at the moment of fault clearance, unlike other existing FRT schemes wherein this is dissipated in the resistors of the crowbar circuit. This results in achieving rotor speed stability, reduced rotor speed deviation and electromagnetic torque fluctuation. Consequently, less reactive power requirement is needed and rapid reestablishment of terminal voltage is attained on fault clearance. Moreover, as the stored energy in the inductor of the proposed scheme is utilized for charging the dc link capacitor on fault clearance, the grid side converter is relieved from charging the dc link capacitor and it can be utilized to its full capacity for rapid restoration of terminal voltage. The simulation results vividly demonstrate the enhanced performance capabilities of proposed FRT scheme employed for DFIG based wind farms.

APPENDIX A. DFIG PARAMETERS

Rated power	(9/0.9) MVA
Angular moment of inertia	0.0887 Kg.m ²
Nominal rms voltage	580 Volt
Base angular frequency	377 rad/s
Magnetizing reactance	4.35 H
Mechanical damping	0.00478 N.m./rad./s.
Stator to rotor turns ratio	2.63
Stator resistance	0.104 Ω
Wound rotor resistance	0.0743 Ω
Stator leakage reactance	2.54 H
Rotor leakage reactance	2.31 H
DC link capacitance	6*10000e-6 F

REFERENCES

- [1] Carrasco JM, Franquelo LG, Bialasiewicz JT, Galvan E, Portillo Guisado RC, Prats MAM, et al. Power-electronic systems for the grid integration of renewable energy sources: a survey. *IEEE Trans Ind Electron* 2006; 53: 1002-16.
- [2] Datta Rajib, Ranganathan VT. A method of tracking the peak power points for a variable speed wind energy conversion system. *IEEE Trans Energy Conver* 2003; 18: 163-8.
- [3] Koutrolis E, Kalaitzakis K. Design of a maximum power tracking system for wind energy conversion applications. *IEEE Trans Ind Electron* 2006; 53: 486-94.
- [4] Srinivasa Rao S, Murthy BK. A new control strategy for tracking peak power in a wind or wave energy system. *Renew Energy* 2009; 34: 1560-6.
- [5] Pena R, Clare JC, Asher GM. Doubly fed induction generator using back-to-back PWM converters and its application to variable-speed wind-energy generation. *IEE Proc Elect Power Appl* 1996; 143: 231-41.
- [6] Grid code regulations for high and extra high voltage Report ENENARHS2006, E.ON, Netz GMBH, Germany 1 (April) (2006) 46 (www.eon-netz.com).
- [7] Piwko Richard, Miller Nicholas, Thomas Girard R, MacDowell Jason, Clark Kara, Murdoch Alexander. Generator fault tolerance and grid codes. *IEEE Power Energy Mag* 2010; 8: 19-26.
- [8] Sun T, Chen Z, Blaabjerg F. Voltage recovery of grid connected wind turbines with DFIG after a short circuit fault. 35th Annual IEEE power electronics specialists' conference. Germany: Aschen; 2004. p. 1991-7.
- [9] Holdsworth L, Wu XG, Ekanayake JB, Jenkins N. Comparison of fixed speed and doubly-fed induction wind turbines during power system disturbances. *IEE Proc-Gener, Transm Distrib* 2003; 150: 343-52.
- [10] Hansen Anca D, Michalke Gabriele. Fault ride through capability of DFIG wind turbines. *Renew Energy* 2007; 32: 1594-610.
- [11] Morren Jochen, De Haan Sjoerd WH. Ridethrough of wind turbines with doubly fed induction generator during a voltage dip. *IEEE Trans Energy Conver* 2005; 20 : 435-41.
- [12] Seman Slavomir, Niiranen Jouko, Arkkio Antero. Ride-through analysis of doubly fed induction wind power generator under unsymmetrical network disturbance. *IEEE Trans Power Syst* 2006; 21 : 1782-9.
- [13] Dittrich Andreas, Stoev Alexander. Comparison of fault ride-through strategies for wind turbines with DFIM generators. In: *Proceeding of European conference on Power electronics and applications*, 11-14 September 2005.
- [14] Chee-Mun. Ong", *Dynamic Simulation Of Electronic Machinery using Matlab/Simulink*", PRINTICE HALL, (1998).
- [15] Pete. Vas " , *Vector Control Of AC Machines*", Oxford University, UK.
- [16] Krause Paul C, Wasynczuk Oleg, Sudhoff Scott D. *Analysis of electric machinery and drive systems*. 2d ed., Piscataway (NJ, USA); IEEE Power Engineering Society, Wiley interscience, John Wiley & Sons Inc 2002.
- [17] Joshi Nitin, Mohan Ned. A novel scheme to connect wind turbines to the power grid. *IEEE Trans Energy Conver* 2009; 24 : 504-10.
- [18] Rahul S . Chokhawala, Jamie Catt, Laszlo Kiraly. A Discussion on IGBT Short-circuit Behavior and Fault Protection Schemes. *IEEE Transactions on industry applications*, Vol. 31, No. 2, Marcw APRIL 1995.

- [19] Chen Z, Hu Y, Blaabjerg F. Stability improvement of induction generator based wind turbine systems. *IET Renew Power Gener* 2007; 1: 81-93.
- [20] Akhmatov V. Variable speed wind turbines with doubly fed induction generators, Art IV: uninterrupted operation features at grid faults with converter control coordination. *Wind Eng* 2003; 27: 519-29.
- [21] Qiao Wei, Venayagamoorthy Ganesh Kumar, Harley Ronald G. Real-time implementation of a statcom on a wind farm equipped with doubly fed induction generators. *IEEE Trans Ind Appl* 2009; 45: 98-107.
- [22] Siegfried Heier, "Grid Integration of Wind Energy Conversion Systems", ISBN 0-471 97143- X, John Wiley & Sons Ltd, (1998).